FAIRCHILD HILLER

FABRICATION FEASIBILITY STUDY OF A 30 WATT/POUND ROLL-UP SOLAR ARRAY

FIRST QUARTERLY REPORT

REPORT NO. 652-00101-QR

OCTOBER 15, 1967

PREPARED FOR THE

JET PROPULSION LABORATORY OF THE CALIFORNIA INSTITUTE OF TECHNOLOGY

UNDER CONTRACT NO. 951969

BY

FAIRCHILD HILLER CORPORATION
SPACE & ELECTRONICS SYSTEMS DIVISION
GERMANTOWN, MARYLAND

FAIRCHILD HILLER CORPORATION

DATE October 15, 1967

SPACE and ELECTRONICS SYSTEMS DIVISION

Germantown, Maryland

DOCUMENT NO.

652-00101-QR

TITLE

First Quarterly Report

Fabrication Feasibility Study of a 30 watt/ Pound Roll-up Solar Array

Contract No. 951969

No. Pages 86

PREPARED _____ ORIGINATOR

APPROVED _____ QA/REL/MAINT

APPROVED _____ MANUFACTURING

APPROVED _____ SPECS. & STDS.

APPROVED _____ ENGINEERING

APPROVED _____ PROGRAM

APPROVED _____

APPROVED _____

REVISIONS

"This work was performed for the Jet Propulsion Laboratory, California Institute of Technology, as sponsored by the National Aeronautics and Space Administration under Contract NAS 7-100."

"This report contains information prepared by Fairchild Hiller Corporation under JPL subcontract. Its content is not necessarily endorsed by the Jet Propulsion Laboratory, California Institute of Technology, or the National Aeronautics and Space Administration."

ABSTRACT

This is the First Quarterly Report required by JPL Contract No. 951969 for a Fabrication Feasibility Study of a 30 Watt/Pound Roll-Up Solar Array. This study includes the parametric investigation of factors effecting the power/weight ratio and concentrates attention on the deployment/retraction mechanisms and supporting structures rather than on the electrical aspects of the design. Preliminary parametric study results are presented as are also conceptual designs of components for two array supporting structure configurations.

This report covers the activity between June 27, 1967 and September 30, 1967.

TABLE OF CONTENTS

GLOSSARY

TEE -- Tubular Extendible Element: a tubular element composed of a metallic, or other material, ribbon exhibiting memory characterisitcs and which is so formed as to stake, in the unstressed configuration, the shape of a long slender tube. The element may be flattened and elastically stressed in a manner to permit its storage on a drum of small diameter relative to the element length.

1.0 INTRODUCTION AND SUMMARY

1.1 Introduction

This document presents the results of the first quarter of a one-year study contract to evaluate the feasibility of fabricating a 30 watt/pound or greater roll-up solar array. The work was conducted by the Fairchild Hiller Corporation, Space and Electronics Systems Division, for the Jet Propulsion Laboratory, California Institute of Technology, under Contract Number 951969. The report covers the period between June 27, 1967 and September 30, 1967.

The objective of the study is to determine the feasibility of fabricating a 30 watt/pound or greater roll-up type solar array and is constrained to the use of technology which can be reduced to practice no later than June 1969. General requirements for the design are presented in JPL document 501407, Revision A, entitled "Detail Requirements for a 30 Watt/Pound Roll-Up Solar Cell Array." The contract also includes requirements that the array be capable of both deployment and retraction, and that a scale model array be fabricated which is capable of demonstrating the deployability of the design concept. The array design shall be based upon an area of 250 square feet.

1.2 Summary

The design of any solar array may be logically divided into two main categories: (1) electrical design which is concerned primarily with solar cell performance under the specified conditions and the associated electrical circuitry and physical layout of the cells on the panel; (2) the design of the supporting structure which includes a panel substrate deployment mechanism and associated structural and mechanical elements. The emphasis in this study is on the structural and mechanical aspects of the design rather than on cell performance, which has been covered in considerable depth in other investigations. The electrical aspects of the design will be studied only to that extent necessary to understand the impact of the electrical parameters upon the overall system design.

The philosophy followed in the conduct of this study has been one of identifying those factors which may have a direct bearing upon the power/weight of the panel design, and through parametric investigations of these factors, establishing the significance of each parameter. As detailed parametric information is generated, system studies will be conducted relating the effects of each factor upon the overall system. The system studies are directed towards establishing a design which provides a maximum power/weight ratio of the overall system.

During the first quarter, a detailed program plan was generated and submitted to JPL for approval. Upon their recommendation, the plan was revised, resubmitted, and approved towards the end of the second month. Following approval of the plan, detailed investigations were initiated.

The major effort during the last third of this quarter has been directed towards generation of conceptual designs of various details of two basic approaches of a structure capable of extending and supporting the array panel. One design employs a folding arm concept with programmed joint motion to ensure straight line deployment of the panel. The second design uses tubular extendible elements (TEE) which is being studied in two configurations. One TEE is a metallic ribbon formed into an overlapping, open section tube. In the retracted mode, the tubular element is flattened out and rolled upon a storage drum. The second approach employs the Fairchild Hiller Hingedlock concept of two flat ribbons which have been formed into a semicircular cross section and interlocked along their edges mechanically to provide, in the deployed position, a closed tubular element. During retraction, the surfaces are pressed together, pivoting about their hinged intersection and stored upon a circular drum.

The aspect ratio of the deployed array (length vs. width) has a fundamental effect upon the design of the various components. Using 250 square feet as a base line for the surface of the panel, it is possible to develop various combinations of length and width and to investigate these effects upon the design of the detailed parts. The maximum width of the array is established by the available volume within the shroud launch vehicle as defined in the contract specification. A practical maximum width is 12 feet. Hence the minimum length of the array is on the order of 24 feet. For a

minimum width of the array of six feet, the length of the array will be on the order of 45 feet. Consequently, these values have been used as practical limits of the array dimensions. It is obvious that a narrower and longer array is possible; however, such a design will result in lower natural frequencies of the array and pose a storage problem for the very long array and supporting arm structure. Since it is impossible within the scope of this study to investigate the extreme limits of all possible combinations of all design parameters, practical limits must be established through good engineering judgment. This philosophy has been followed in the study.

The structural mechanic/dynamic studies conducted to date have established a natural frequency of the panel substrate assemblies (including substrate and cell stack assemblies) as functions of substrate tension, substrate mass loading per square foot, and panel length which is a function of panel aspect ratio. It is shown that the minimum acceptable natural frequency of 0.04 Hz may be achieved for all practical aspect ratios of the panel with moderate substrate tension loads.

The substrate tension loads impose a column load upon the panel extension/supporting structure. Using these loads with anticipated reasonable eccentricities, both the folding arm and TEE device supporting structures have been investigated parametrically to establish reasonable design dimensions for three materials each. Materials investigated to date include aluminum, titanium, and stainless steel for the folding arm design, and beryllium copper, stainless steel, and titanium for the TEE devices. Other high modulus/weight materials will be investigated the next reporting period.

Since solar cell power output is related inversely to solar cell temperature, the initial thermal dynamic studies have investigated possible methods of reducing cell temperatures through the use of thermal control coatings on both the forward (sun) side and reverse side of the panels. It is concluded that cell temperatures may be reduced a few degrees through the use of thermal control coatings in the spaces between cells and covering the cell interconnection wiring, the improvement in power output of the system will be on the order of 1-1/2 percent. However, this improvement in performance can be attained only through development of methods of application for such coatings and probably will require very complicated production techniques. On the other hand, the use of thermal control coatings on the anti sun-side of the

substrate appears feasible.

Materials investigations to date have included some preliminary tests on the creep rate of Kapton H film which is proposed as a substrate material. Design allowables of candidate materials for the structural members are being compiled.

The array supporting members (folding arm and TEE's) are designed primarily by the applied column and bending moment loads in the fully deployed position. Therefore, high modulus/weight materials exhibit a distinct advantage in this application. Composite materials employing boron filaments or beryllium wire in a plastic matrix appear quite attractive for this application. Design allowables for these materials are being obtained from manufacturers of such composites and are expected to be augmented through laboratory tests conducted by Fairchild Hiller.

Electrical studies are being conducted to determine the maximum power/weight design available as a function of cell thickness. The study, however, has not progressed to a point where meaningful results can be reported.

2.0 TECHNICAL DISCUSSIONS

During the first quarter of the program, the primary effort has been directed along two lines; (1) the generation of conceptual designs of the system as a whole and of its components, and (2) parametric investigations of significant factors. Investigations have been of a broad general nature with emphasis placed upon identifying areas requiring study and gaining preliminary knowledge of the effects the various parameters will have upon the design.

It must be recognized that the selection of an optimum system may require compromise in the selection of the various components. A complete and thorough understanding of the effects of variations of parameters within each of the subsystems (i.e. structural design, electrical design, structural and materials analyses, etc.) is essential to the conduct of trade studies. Therefore, the system analyses efforts during this period have been directed primarily toward establishing practical limits for the parameters under investigation by the various functional groups.

Detail systems analyses, which will integrate the results of the parametric studies conducted during the first quarter and which will continue through the second quarter, will be conducted during the following reporting period and will result in the selection of a maximum power/weight ratio design.

2.1 STRUCTURAL DESIGN

A systematic investigation was begun of those parameters which would aid in the selection of an optimum design of a 30 watt/pound roll-up solar array.

Design concepts for various constituent parts of the overall system were formulated and will continue to be formulated during the course of this study

The structural/mechanical design of the solar array is divided into sub-classifications as noted below:

- Structural Housing
- Drive, Extension & Retraction System
- Extension and Retraction Mechanism
- Release System
- Damping System
- Panels

Each sub-classification is further divided into detail parts as required Design concepts are being formulated for each detail part. These concepts consist of all ideas which may be feasible, regardless of how extreme the concept may seem.

A comprehensive parametric investigation has been initiated and is continuing with each of these detail parts in order to assess the feasibility of the concept and to permit identification of the optimum design approach

Using 12, 7.6 and 6 foot wide arrays and the single link folding arm as a basis for initial investigations, preliminary packaging arrangements were formulated. Preliminary volumes for these arrangements were also determined, and are given in Table 2.1.1

All of the formulated design concepts are being parametrically studied and will encompass electrical and mechanical design factors, materials application and configuration variations.

The structural/mechanical design approach employs systematic investigations of all design concept details using configuration parameters which affect the power/weight ratio of the overall array system.

TABLE 2.1.1

PACKAGING VOLUMES

FOLDING ARM STRUCTURE

ARRAY WIDTH (IN)	ARM ELEMENT MAX. LENGTH BETWEEN JOINTS	VOLUME (CU. FT.)
72	78	25.0
72	137	20.0
90	91	23.1
144	149	22.3

TEE HINGELOCK TUBE

ARRAY WIDTH (IN)	CRITERIA	VOLUME (CU. FT)
72	Nominal Packaging *	19.2
72	Minimum Eccentricity **	19 9
72	Minimum Package Vol.	16.6
90	Nominal Packaging	20.7
90	Minimum Eccentricity	21.7
90	Minimum Package Vol.	18 2
144	Nominal Packaging	28.5
144	Minimum Eccentricity	30.0
144	Minimum Package Vol.	25.4

* Nominal Packaging: Realistic packaging without crowding permitting ease of maintenance and assembly.

** Minimum Eccentricity: Refers to angle between panel and TEE structure Minimum eccentricity results in minimum bending load applied to TEE in extended position by panel substrate tension.

These parameters will include but are not limited to:

- weight
- volume
- cost
- structural soundness
- reliability
- repeatability (alignment accuracy)
- ease of manufacturing
- growth capability

The following sections define the various components of the general system approach and conceptual designs for each system which is being studied.

2 1.1 Structural Housing

The purpose of the structural housing for the roll up solar array is to support the mechanisms and the substrate from loads induced by vibration, handling, launch, maneuvering and thermal gradients The structure will be rigid enough to insure deployment and retraction without binding of the mechanisms. The materials for the structure will be non-magnetic, compatible with a space environment and will possess a high strength to weight ratio.

The structural housing sub system was broken down into the following detail parts:

- Substrate support roller
- Foam backing take-up roller
- Spreader bar
- Base support structure
- Roller support brackets
- Top, bottom and back plate
- Handling fixture

The methods of fastening under consideration for any of the structure are: welding, which may cause distortion; bonding, which require expensive tooling but gives uniform joints and is ideal for thin sheets; mechanical fasteners, which includes screws, bolts, rivets and similar devices.

2.1.1 1 Substrate Support Roller

The substrate support roller contains no flanges since they would tend to scrub the edges of the substrate during deployment/retraction and possibly result in damage to the substrate. Since the array will contain a foam backing while in the rolled position, flanges on the support roller are not required to support the array during vibration. The foam will provide a damping action.

The substrate roller may be made in one piece or multi-sectioned. It is felt that a multi-sectioned (2 or more) roller will result in a lighter weight design; this approach is being studied

The conceptual designs formulated thus far are:

- Hollow tube
- Spoke webs - longitudinal webs in a hollow tube.
- Bulkheads and stiffening rings - strategically placed along the length and inside a hollow tube roller
- Bulkhead and stringer - aircraft type construction with longitudinal stringers and ring type bulkheads mounted in a hollow tube
- Honeycomb sandwich - lightweight honeycomb with thin face skins formed into a cylindrical shape
- Rigid Polyurethane - rigid polyurethane foam either inside a hollow tube or formed outside a small dia. hollow tube
- Tube with BeCu skin - Hollow tube with BeCu skin wrapped around it (this skin may have some later use as a substrate tensioning device)
- Solid rod - solid roller with many longitudinally cored holes for lightness.

Figure 2.1.1 illustrates these concepts

In selecting the final roller concept lightweight design will be a prime consideration. This will be accomplished thru lightening holes in the roller tubes, the use of lightweight materials, or a combination of these methods

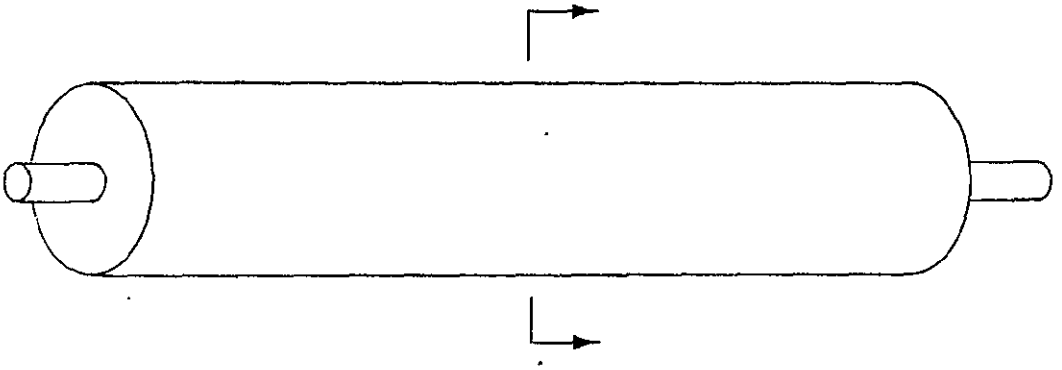

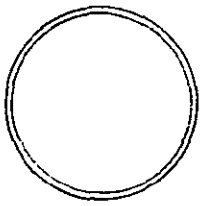

HOLLOW TUBE

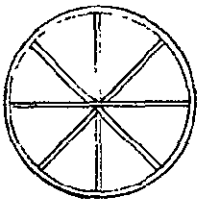

SPOKE WEBS WITH TUBE

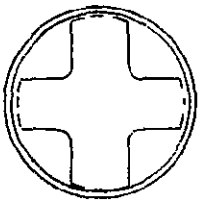

BULKHEAD SUPPORTS

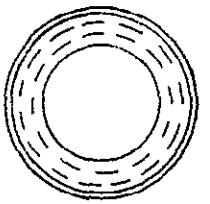

STIFFENING RINGS

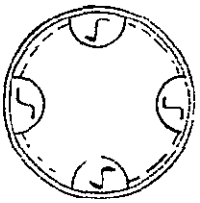

BULKHEAD & STRINGER

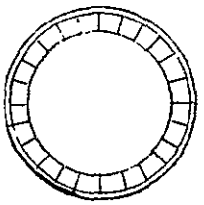

HONEYCOMB SANDWICH

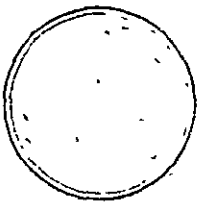

RIGID POLYURETHANE FOAM INSIDE TUBE

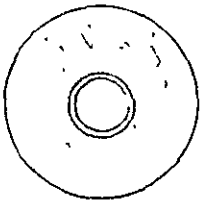

RIGID POLYURETHANE ON OUTSIDE OF SMALL TUBE

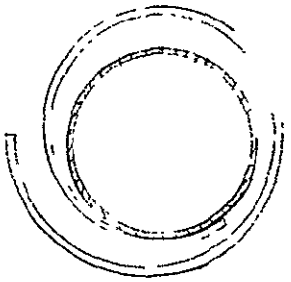

TUBE WITH FURLED B_e C_u SKIN

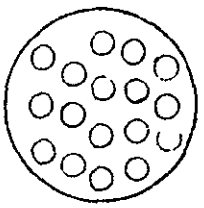

SOLID ROLLER CORED FOR LIGHTNESS

SUBSTRATE ROLLER
FIG. 2.1.1

Some of the materials under investigation for the roller are:

- Aluminum
- BeCu (Beryllium Copper)
- Fiberglass
- Boron filled fiber glass
- Magnesium

Among the support roller parameters being investigated are; variations in roller materials, length, diameter, roller thickness and number of support points.

2.1.1.2 Foam Backing Take-Up Roller

To prevent scuffing of the cells and coverglass breakage, an open cell polyurethane foam is interleaved between the cell layers. This foam may be either attached to the substrate back or stowed seperately on its own take-up roller A trade off study is being performed to compare the weight of a foam take up mechanism vs. the weight of adhesive required to bond the foam to the substrate back, plus the additional cells required due to thermal considerations.

The foam take up roller design concepts are identical to those for the substrate roller except the foam roller will be a much smaller diameter since it need support only its own weight during launch and the lightweight foam after deployment.

2.1 1.3 Spreader Bar

The spreader bar spans between the two (2) support plates for the substrate roller and provides a mounting surface for the outboard end of the substrate, as well as an attachment point for the deployment linkage It also retains the deployment mechanism during launch.

The basic design concepts for the spreader bar are:

- Sheet metal
- Honeycomb
- Corrugated

- Rigid polyurethane core and skin
- Machining or casting

Figure 2.1.2 shows the basic design shape which is similar for all types of construction.

Flat sheet metal spans are inadequate for vibration unless stiffeners are added. Machined parts are made lightweight by the elimination of overlapping webs and fittings and can be stiffened with integral machined web stiffeners They are, however, relatively expensive. Honeycomb structure is generally lightweight but sometimes difficult to attach to adjacent parts. Lightweight fittings usually are difficult to achieve with truss designs. All of these aspects are being investigated.

The materials under investigation for the spreader bar are the same as those mentioned in Section 2 1 1 1.

2.1.1.4 Base Support Structure (Side plate)

This piece of structure is the attaching interface to the spacecraft and is the principal load carrying member. It will be bolted directly to the spacecraft structure and will support the deployment, retraction, release mechanisms, substrate and foam rollers. The side plates will be either a single plane or a multi-plane overhanging part, depending on the length of the substrate The overhanging part will be required in cases where the substrate width is wider than the mounting surface for the array. Figure 2.1.2 shows a general design for the overhanging type structure. The shape will remain the same regardless of the type of construction.

The materials under consideration are the same as those mentioned in Section 2.1.1.1.

The design concepts formulated for consideration at this time are:

- Machining or casting
- Honeycomb
- Sheet metal and stiffeners
- Tubular truss
- Laminated Fiberglass

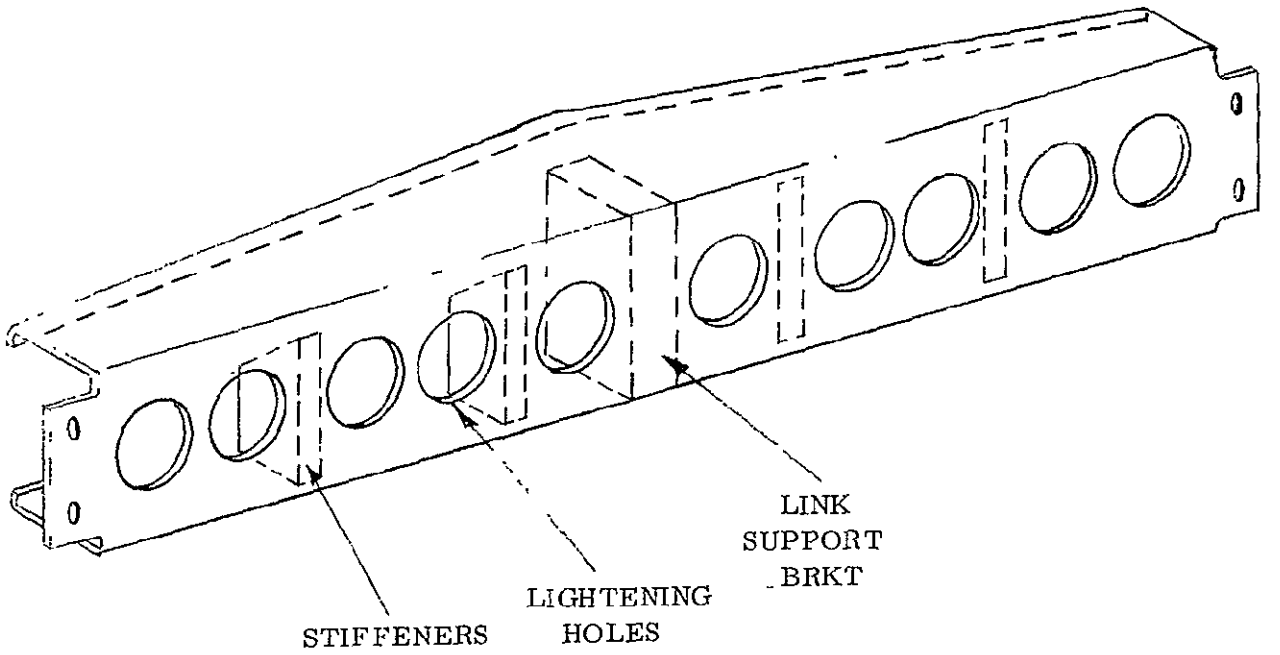

SHEET METAL & STIFFENERS
SPREADER BAR

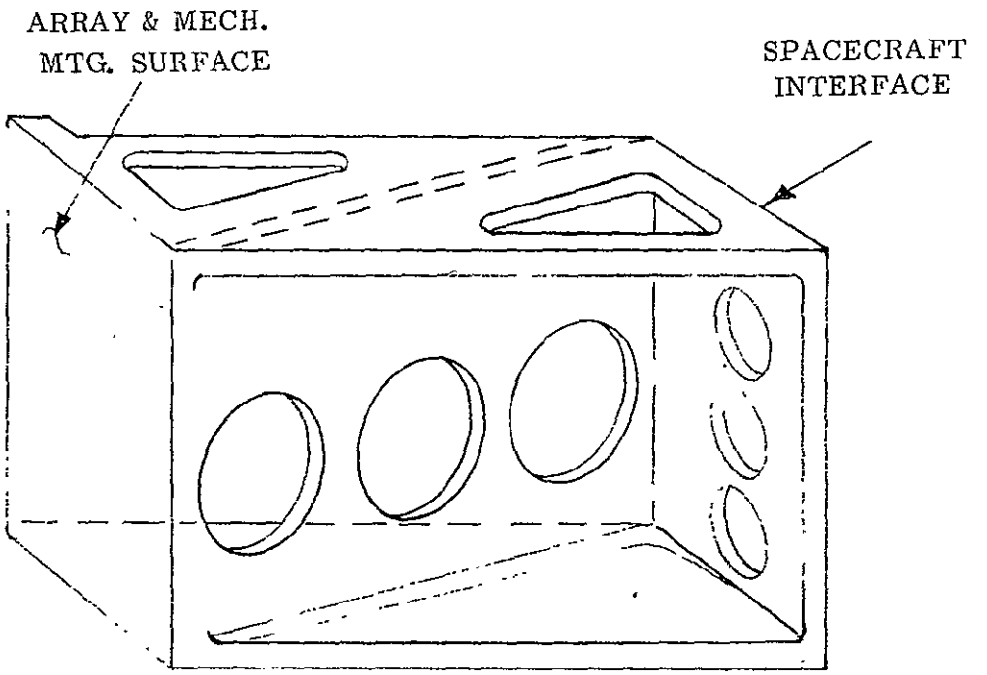

BASE SUPPORT STRUCTURE

FIG. 2.1.2

The advantages and disadvantages of these fabrication methods are the same as those discussed under Section 2.1.1.3. Spreader Bar design.

A first look at this design seems to indicate that a magnesium machined part will be best because of its lightness, strength and easy machinability.

2.1 1.5 Roller Support Brackets

The initial examination of the substrate support roller design indicate that the lightest and strongest roller will be a multi-section design (two or more sections). In the event a sectioned roller is used, additional roller support brackets will be required These brackets will serve as intermediate supports for the roller and will attach through the structure back plate (if one is required) and into the spacecraft mounting area.

The material selection manufacturing techniques and detail design will be similar to those noted in Section 2 1.1.4 Base Support Structure-Preliminary appraisal indicates that the most favorable design would be a machined fitting

2.1.1.6 Top, Bottom and Back Plate

In order to provide load carrying capability to the structural housing it is necessary to add a top and bottom plate to the box. These plates span the gap from one side plate (base support structure) to the other and are fastened to the side plates. The conceptual designs formulated for the top and bottom plate, the materials and manufacturing techniques are very similar to those of the spreader bar (Section 2.1.1.3). Here again the design approach is that which results in the best strength to weight ratio. At a later date in the design investigation it may be discovered that the top and bottom plates will have to serve as mounting surfaces for the roller brackets (intermediate supports noted in Section 2.1.1.5). With this design approach it may be possible to eliminate the back plate, which would be used only for stability and handling and not as a structural member The back plate, if used, will be thin, lightweight sheet metal reinforced with lightening holes and/or beads.

2.1.1.7 Handling Fixture

Since the array structural housing (box) is of such great length (from 6 feet to 12 feet), it was necessary to consider a handling fixture for use with the array system. This fixture will be long enough to span from one side plate to the other and will be attached to the array system during all ground testing and handling. The fixture will be removed upon installation of the array system into the spacecraft. If it is ultimately decided to use the handling fixture, then the back plate, mentioned in Section 2.1.1.6, will not be required; thereby resulting in a weight savings.

Since this fixture will be used only for ground support, weight is not a prime consideration; thus, it can be made strong enough to withstand the loads encountered during testing and handling. It will be designed for easy installation and removal and to clear all adjacent structures in the spacecraft. The fixture will contain hand holds for easy handling and will be designed to remain in place during array checkout.

2.1.2 Drive, Extension and Retraction System

The drive, extension and retraction system was divided into the following categories:

- Folding arm linkage
- TEE (Tubular Extendible Element) devices
- Extension and retraction mechanisms
- Synchronizing system

These deployment and retraction concepts were chosen for further study with a flexible substrate system.

2.1.2.1 Folding Arm Linkage

Two mechanical folding arm linkage design concepts were formulated. They are:

- Tubular single link
- Scissors linkage

Figure 2.1.4 shows these concepts.

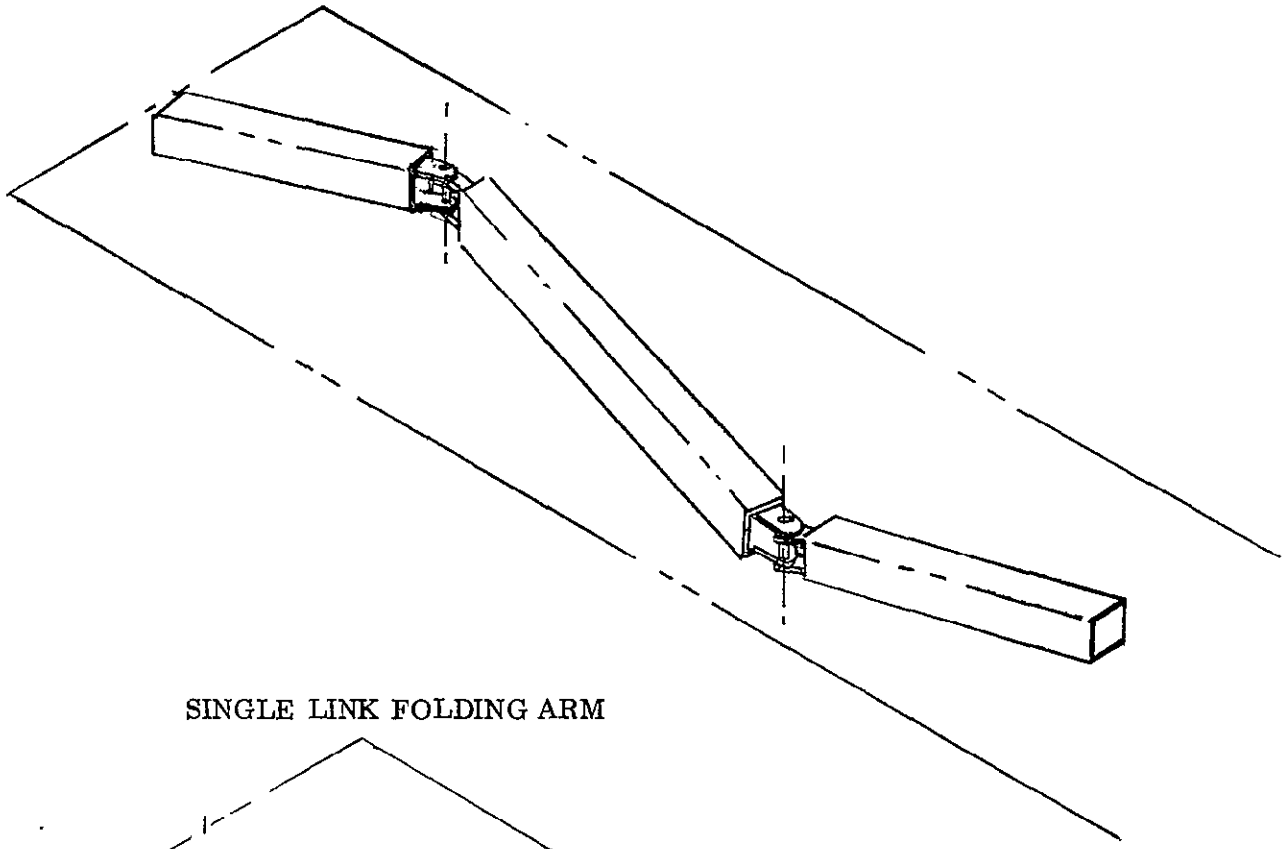

SINGLE LINK FOLDING ARM

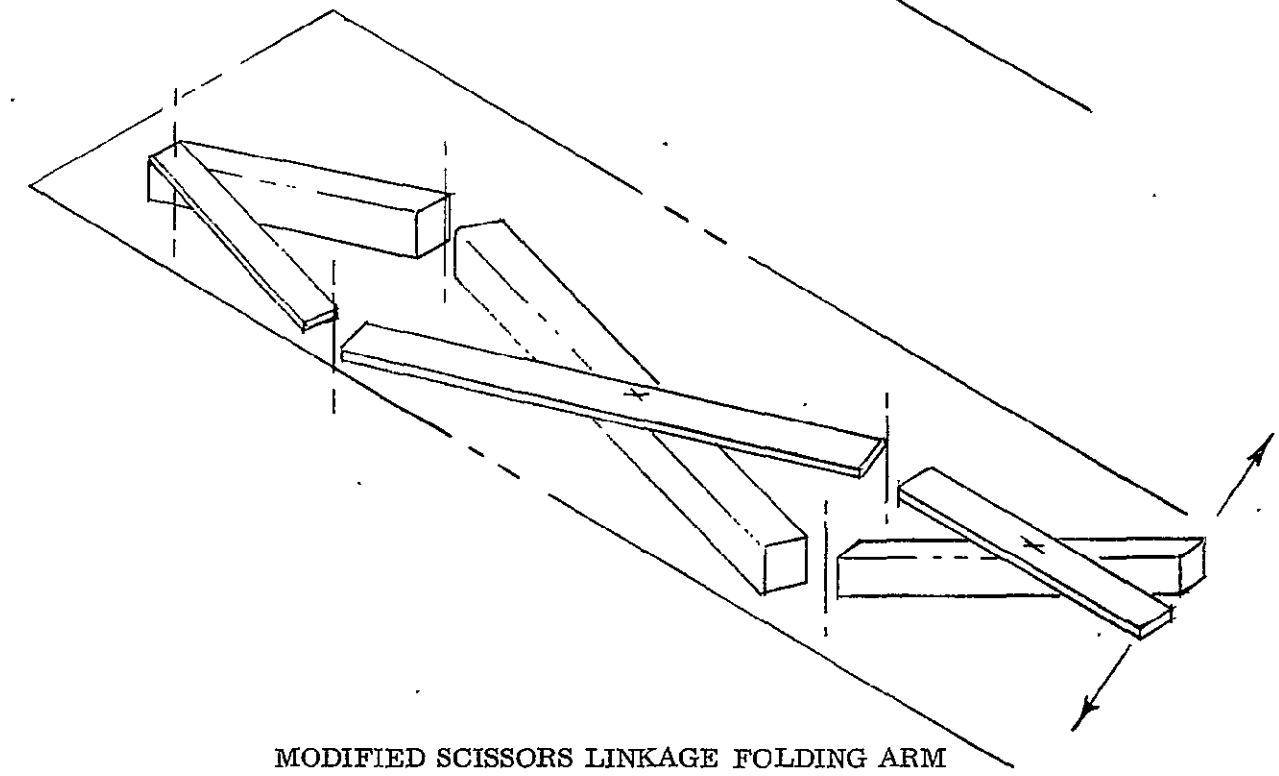

MODIFIED SCISSORS LINKAGE FOLDING ARM

FIG. 2.1.3

Tubular Single Link

The design is composed of hinged arms mounted to the base structure and deploying outward with a straight line motion at the tip. This straight line motion is obtained by cables, pulleys and auxiliary gearing mechanisms which control the rate of deployment at the joints.

Scissors Linkage

A modified scissors linkage is used which does not require a rate controlling system of cables, pulleys, etc. Straight line deployment is inherent in the design since all the links are fastened together in scissors fashion. A weight trade-off is being conducted to compare this concept with the tubular single link concept.

2.1.2.2 TEE (Tubular Extendible Element)

Two TEE configurations are presently under investigation. They are:

- Overlapping tubular element
- Hingelock collapsing tubular element

Figure 2.1.4 illustrates these concepts. Among the materials being investigated for these approaches are: (1) stainless steel; (2) beryllium copper; and (3) aluminum.

Overlapping Tubular Element

This design incorporates two extendible overlapping tubes fastened at their tips by a spreader bar. A dual system is used to provide torsional capability in the elements. Two extension mechanisms, with a mechanical or electrical synchronizing system, may be required to ensure uniform deployment. Two alternatives being investigated are: one deployment mechanism using two (2) tubular element storage reels with a common drive shaft to provide the synchronization; and two (2) elements, one on top of the other, on the same reel and deployed by the same mechanism.

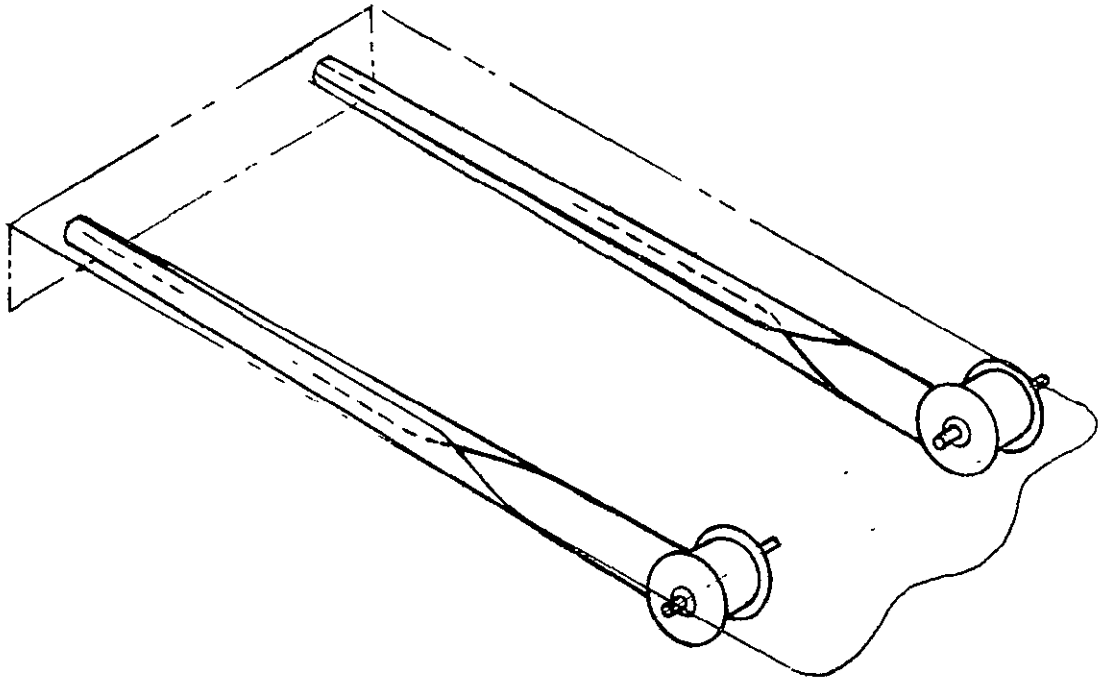

OVERLAPPING TUBULAR ELEMENT

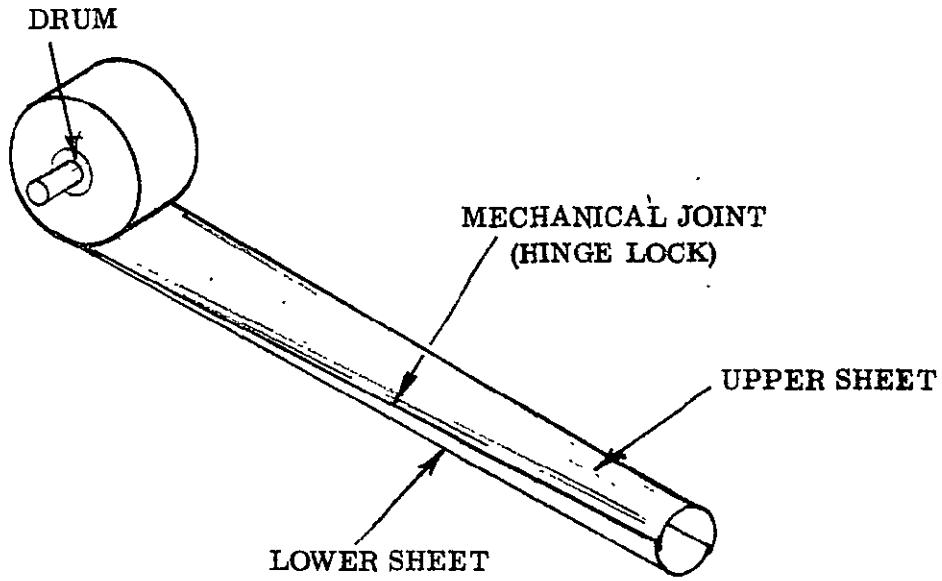

COLLAPSING TUBULAR ELEMENT

FIG. 2.1.4

Hingelock Collapsing Tubular Element

The design consists of two (2) thin curved sheets of metal which are pre-formed to a circular shape and fastened mechanically at the edges using a technique of interlocking tabs and slots. Both sheets, when joined, form a tubular cross section. The tube may be flattened, so that both sheets are in contact over their entire surface, and then rolled onto a storage drum. This method of solar array deployment is being investigated considering both a centrally positioned single tube and two (2) tubes which are located near the edges of the panel.

2.1.3 Extension and Retraction Mechanisms

The methods for extension and retraction under consideration are:

- Screwjack and motor springs
- Direct motor springs
- Pneumatic cylinder
- Torsion springs at hinge joints
- Motor springs with pulley and cable or chain and sprocket
- Combinations of the above
  a. Motor and screw jack
  b. Motor with pulleys and cable

Figures 2.1.5 through 2.1.7 depict these design concepts. Most of these methods will work equally well for both extension and retraction by installing two (2) identical systems, one to drive the deployment system during extension and one to drive the substrate roller for retraction. One half of the system will, however, have to be uncoupled while the other half is operating. Coupling and uncoupling methods are being investigated and if a suitable method can be devised it may eliminate the need for two drive systems.

If two (2) systems are used, it may be possible to utilize the uncoupled system as a substrate tensioning device by the introduction of components such as drag clutches, etc. into the design.

A trade study is being conducted to select the most desirable system for the solary array.

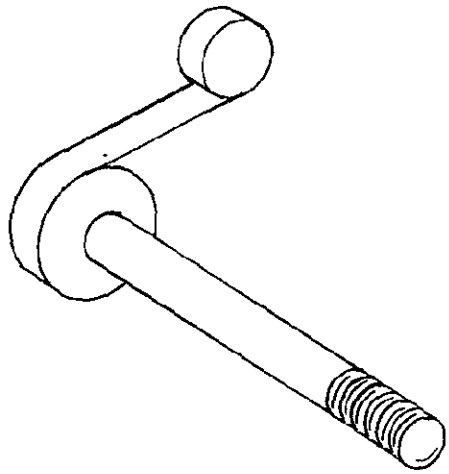

SCREWJACK & MOTOR SPRINGS

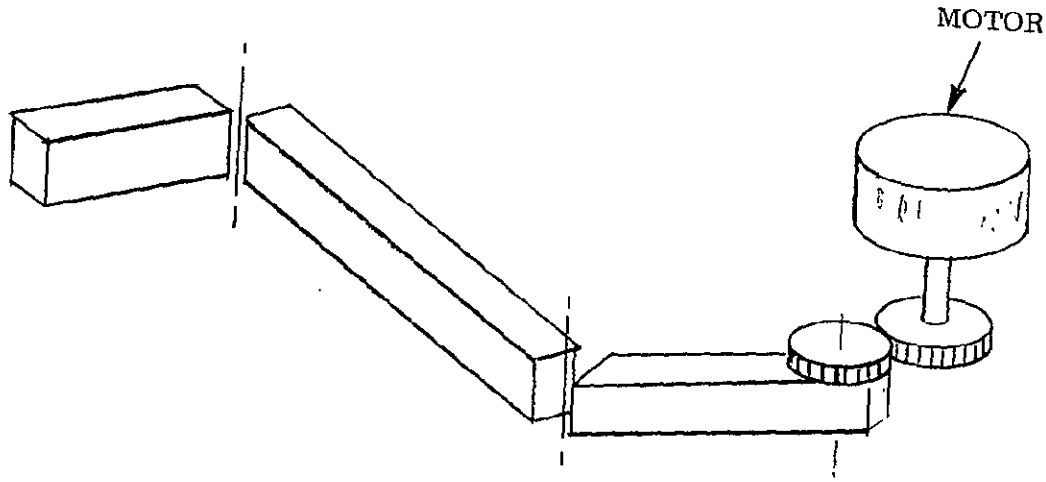

DIRECT MOTOR DRIVE

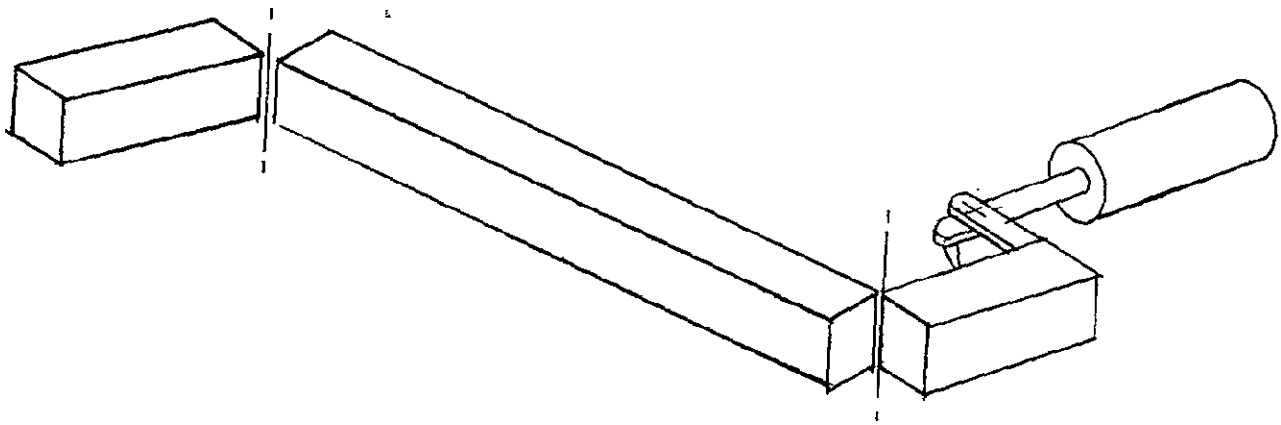

PNEUMATIC CYLINDER

FIG. 2.1.5

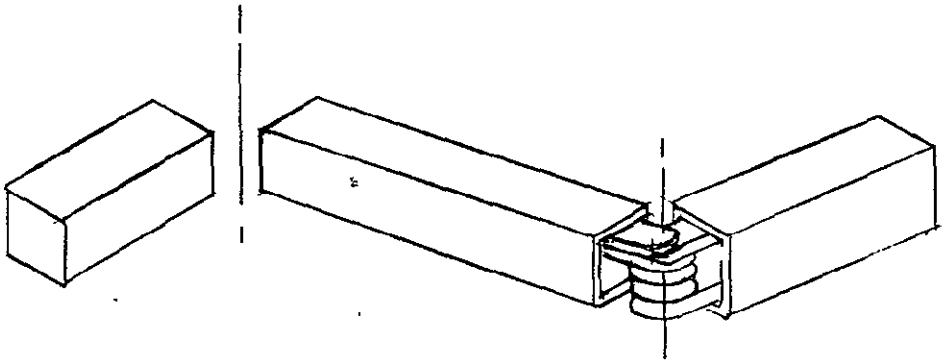

TORSION SPRING

TORSION SPRINGS AT LINK JOINTS

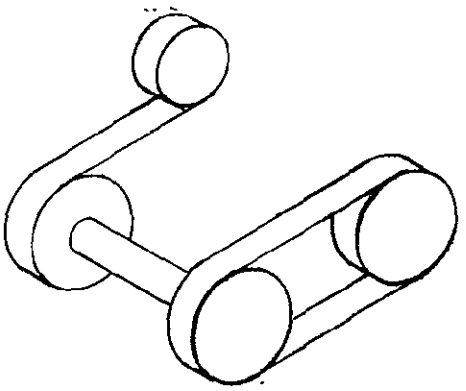

MOTOR SPRINGS WITH PULLEY & CABLE OR CHAIN & SPROCKET

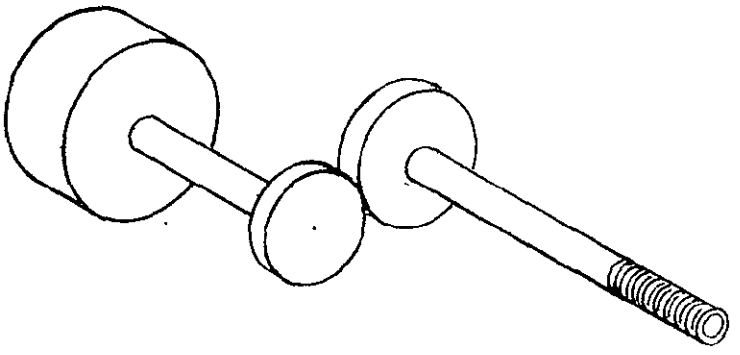

COMBINATION MOTOR & SCREWJACK

FIG. 2.1.6

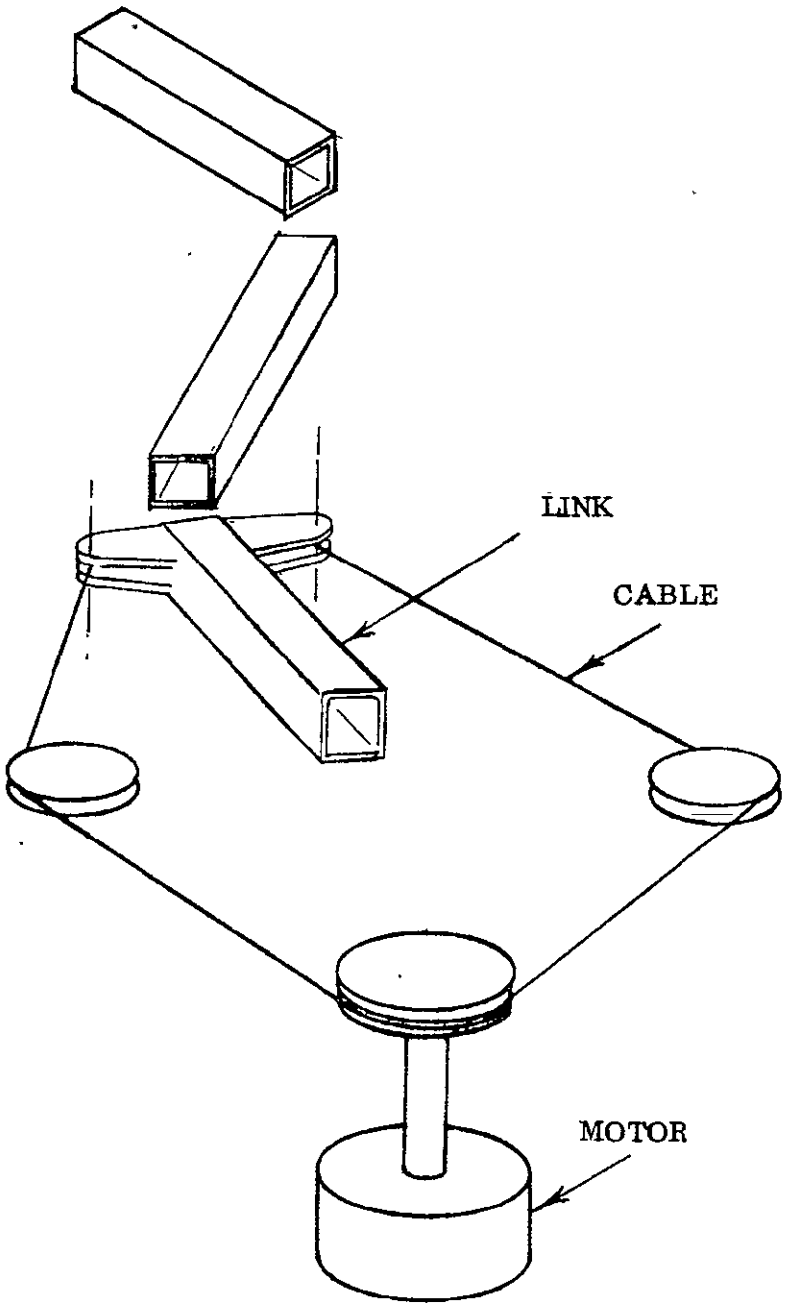

COMBINATION - MOTOR, PULLEYS & CABLE SYSTEM

FIG. 2.1.7 632-00101-QR

2.1.3.1 Synchronizing System

It is normally required to deploy two (2) or more of the solar arrays simultaneously; therefore, synchronizing devices may be required to prevent the introduction of undesirable disturbing torque to the spacecraft. Such devices may be either electrical and/or mechanical.

Candidate design concepts are:

- Bell cranks and push rods
- Pulleys and cables
- Differentials with belts or chain drive
- Right angle gear drives
- Gear and screwjack drive system
- Electrical synchronizing

Bell Cranks and Push Rods

This system would be most useful for linkage type deployment devices. It incorporates a bell crank centrally mounted between the installed solar arrays. Attached to the bell crank are four (4) push rods with each rod extending outward from the bell crank and connecting to the inboard link of the deployment mechanism (the link which attaches to the spacecraft interface surface). Upon rotation of the bell crank each push rod forces the inboard link to translate in such a manner that it causes the solar array to deploy. Reverse rotation causes the solar array to retract.

Pulleys and Cables

A central drive force, such as a motor, with attached cable drum is used for this design. A cable, running from the drum, is routed around pulleys and attached to both sides of the inboard link of the deployment mechanism. Upon rotation of the motor and cable drum, the cable wraps onto the drum while paying out cable from the opposite side of the drum. Drum rotation causes the cable to pull on one side of the mechanism links, causing them to either deploy or retract, depending upon which direction the drum is rotating.

Differentials with Belts or Chain Drive

This system incorporates a drive force which is centrally located between the installed solar arrays. A motor is geared directly to the two (2) differentials which are mounted close by, one for each pair of arrays. The differentials drive a cable and pulley system which is attached to the inboard link of the deployment mechanism. During deployment or retraction, the differentials will compensate for any difference in extension or retraction rates. The system, however, depends upon each array system pair being interconnected through some means, so that there exists a common point of friction. If such is not included the differential will extend or retract the array with the least friction before the other array will be activated.

Right Angle Gear Drives

A gearing arrangement at the corners of the installed arrays is utilized with this system. Each array has a spur-gear mounted to each end of the substrate roller shaft. The array lengths are such that these gears mesh properly with a right angle gear. The rotation of the array roller transmits motion through the roller shaft to the right angle gear, which in turn transmits rotation to the spur gear of the adjacent array, (mounted 90° to the driving array). This design interconnects all four (4) arrays, which are thereby driven simultaneously. The gearing is such that the motive force will drive the links during extension and the substrate roller for retraction.

Gear & Screwjack Drive System

This system is very similar to the right angle gear system described above. It differs in that it is used primarily for a scissors type deployment mechanism. The two (2) inboard links of the scissors mechanism are fastened to a screwjack which in turn is connected to a spur, right angle gear system. The deployment and retraction motions are the same as those with the right angle drive system described above in that the motion is transmitted through a screwjack slide mechanism to a spur, right angle gear combination and to the next array which is mounted 90° to the driving array.

Electrical

An electrical synchronizing system which controls the extension/retraction motors speed through position sensing and feed back control provides a flexible design and uses proven concepts It has the additional advantage over mechanical interconnection of array deployment mechanisms in that deployment malfunction of one array will not prevent operation of the other array mechanisms.

2.1.4 Release System

The release mechanism will support the extension mechanism during vibration, shock and thrust loading and prevent inadvertent deployments. It will be compact and will have fast reaction time so that upon release it allows the substrate to initiate deployment without billowing or snapping that could introduce high shock loads when the linkage overtakes the array panel.

The release system will include two sub-systems:

- Release mechanism for the deployment linkage
- Latching system

2.1.4.1 Release Mechanism

The conceptual design devised for the deployment linkage release system are:

- Clamping hooks mechanism
- Cinch up mechanism
- Spring loaded latches with cables

These mechanisms may all be released by either an electrical device (solenoid) or by a phrotechnic device (cable cutters, pin pullers, etc.)

Clamping hooks

Two sets of clamping hooks are attached to the end plates of the structure. The hooks are positioned over the spreader bar and retain the extension mechanism. Simultaneous release of both sets of hooks is accomplished through solenoid operated sliding cams, push rods and a toggle linkage. The forces thus transmitted to the hooks forces them to rotate open and release the spreader bar. This type system

was used on two (2) previous deployable solar arrays built by FHC and is illustrated in Figure 2.1.8.

Cinch Up Mechanism

This design uses a spring loaded tubular truss type structure that bridges from one side plate to the other. The truss is built as two (2) triangular sections with the base of the triangle attached to the side plates and the apex terminating at a common point in the middle of the spreader bar. The apexes of the triangles are connected with a release device (solenoid or pyrotechnic) which when activated, allows the spring loaded truss to swing out of the way and allows the extension linkage to deploy. This type system was used successfully on the Pegasus spacecraft.

Spring Loaded Latches With Cables

A set of spring loaded "fingers" which reach in front of and retain the spreader bar and deployment linkage are used for this system. The fingers are retained by a cable which is released by redundant cable cutters. Upon release of the cable tension (by cutting), the spring loaded fingers rotate out of the way, thereby freeing the spreader bar. Instead of cables, the fingers may be retained by mechanical components.

2.1.4.2 Latching System

Latches are required in both the extended and retracted positions of the array. Most of the latching methods defined herein can be adapted for use in either configuration position with minimum re-design. Design concepts under consideration are:

- Electro/mechanical latch
  a. Motor driven screwjack and worm gear
  b. Rotating camsand limit switches
  c. Camming latch
- Mechanical spring loaded latch
- Escapement type

  Ratchet and pawl with solenoid pin retention
- Link latches
- Screwjack lock

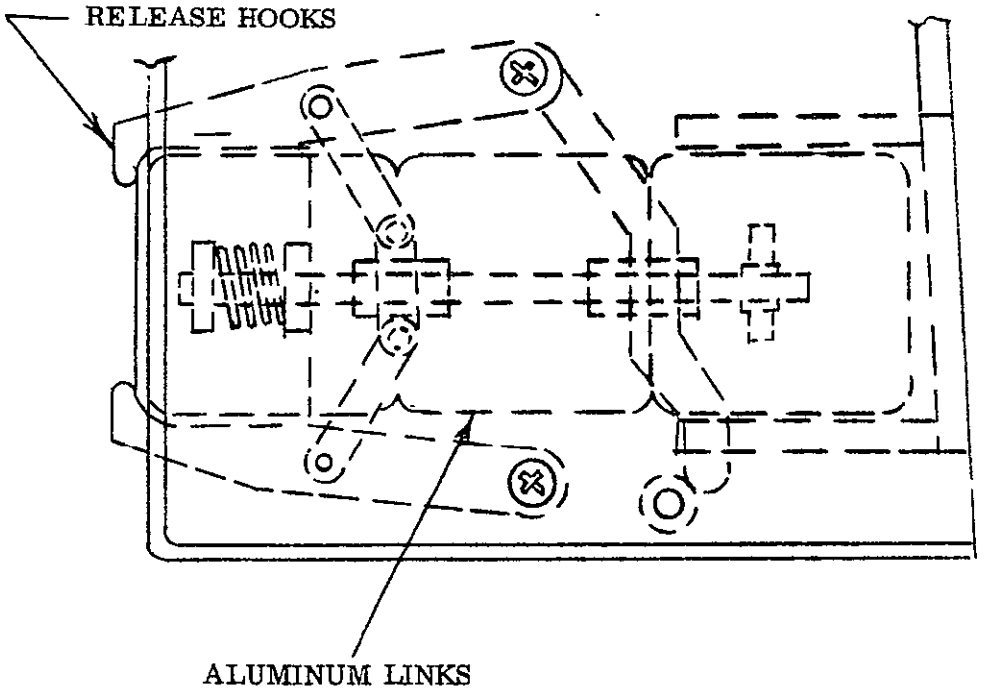

RELEASE MECHANISM

FIG. 2.1.8

Electro/Mechanical Latch

All of these devices use an electrically driven cam device which, upon extension or retraction, grasps a structural protrusion on the deployment mechanism and cams or draws the mechanism down tight. The most promising of numerous variations of this device will be studied.

Mechanical Spring Loaded Latch

Many variations are possible with this mechanism. Basically, all use a spring loaded hook which snaps over a solenoid operated, retractable pin, that holds the hook in place. Retracting the pin releases the hook. The hook will be attached either to the deployment linkage or the side plates depending on whether it is an extension or retraction latch.

Escapement Type

The design uses a ratchet and pawl device which engages at a pre-determined point. The ratchet is locked by a retractable pin.

Link Latches

The latches are of two (2) types, depending on whether the extension and retraction mechanism is a single tubular link or a two (2) element scissors link. The scissors link latch uses a spring loaded hook, which snaps over a retractable pin when the mechanism reaches a predetermined point in its extension or retraction. This concept (also called a joint lock) is shown in Figure 2.1.9).

The Figure 2.1.10 illustrates the tubular link latch. It can also be used for scissors linkage with slight modifications. The latch consists of a protrusion on the inboard link of the deployment mechanism which snaps behind a spring loaded retention fitting. Upon command, an electrically operated solenoid retracts the fitting to release the latch and permit array retraction.

Screwjack Lock

This lock is a device used with a screwjack deployment mechanism which prevents rotation of the screwjack in either direction. It can be a device which locks a gear attached to the end of the screwjack or a retractable, slider lock which is activated by the screwjack slides and retracted by electrical means (such as a solenoid pin).

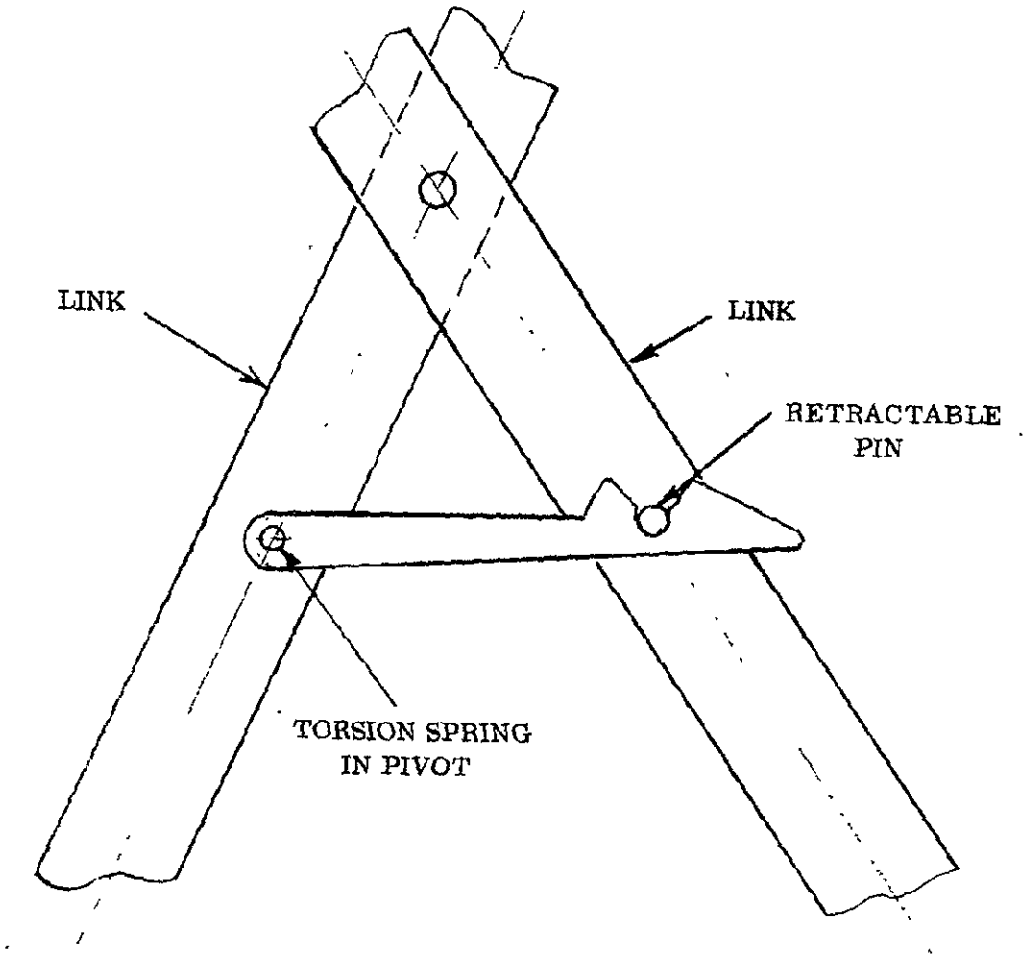

EXTENSION LOCK

FIG. 2.1.9

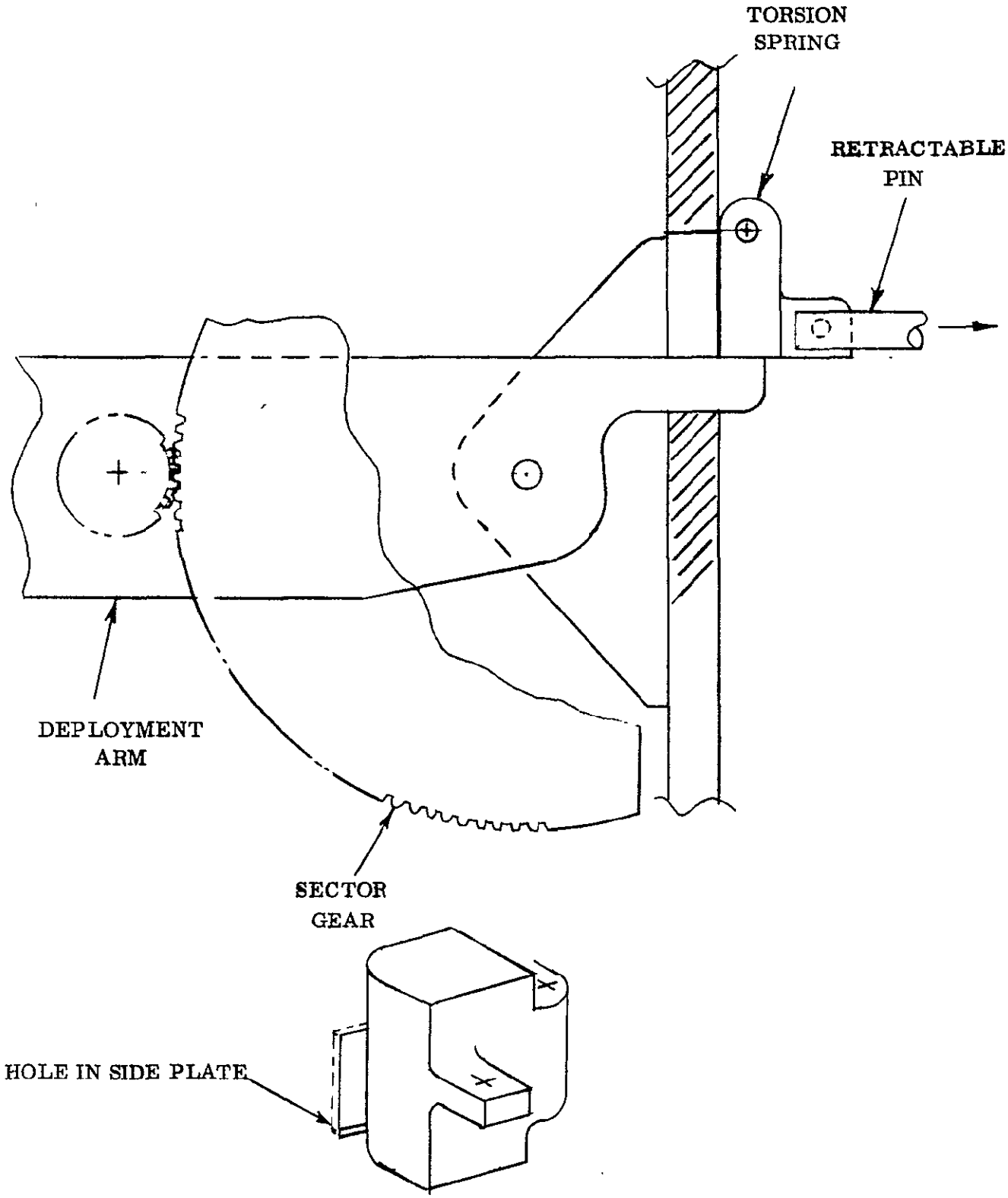
TORSION
SPRING
RETRACTABLE
PIN
DEPLOYMENT
ARM
SECTOR
GEAR
HOLE IN SIDE PLATE

FIG. 2.1.10

2.1.5 Damping System

Deployment rate control is provided by a damping system which is attached to the substrate roller to prevent substrate billowing during deployment. This application requires a rotary damper or one which translates rotary motion to linear motion.

Among the methods being investigated are:

- Centrifugal brake
- Hydraulic or gas cylinder
- Friction brake
- Fluid coupling
- Escapement mechanism
- One way and drag clutches

Figures 2.1.11 through 2.1.14 are illustrations of these concepts.

The centrifugal brake has been successfully used on two previous deployable solar array programs conducted by Fairchild Hiller for the Goddard Space Flight Center of N A S A. Angular velocity imparted to the storage drum by the substrate during deployment is transferred to the flyweights through a high ratio planetary gear train. The flyweights, acting under this rotational influence, cause the attached friction pads to contact the brake drum thus causing a restraining torque to be applied to the storage drum.

The other damping methods mentioned above will be investigated for possible application and compared on the basis of their advantages and disadvantages.

Included in the Damping System is the array tensioning system. Candidate design concepts include:

- Deployment links as a tensioner
- Substrate roller torsion springs
- Array roller with attached motor springs

Figure 2.1.14 depicts the latter concept.

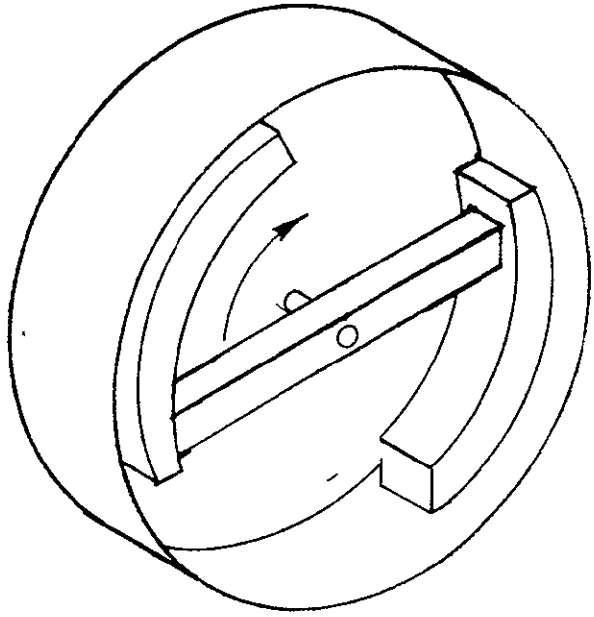

CENTRIFUGAL BRAKE

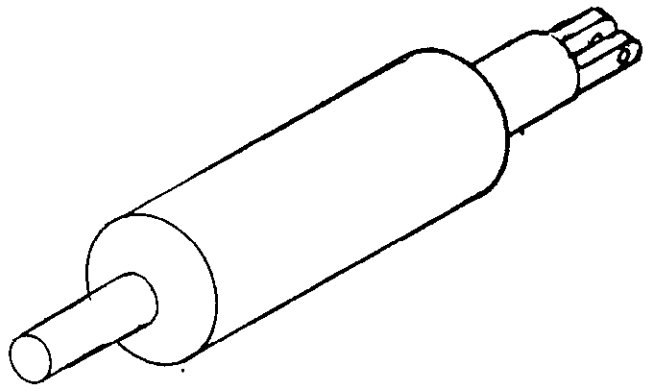

HYDRAULIC OR GAS CYLINDER

FIG. 2.1.11

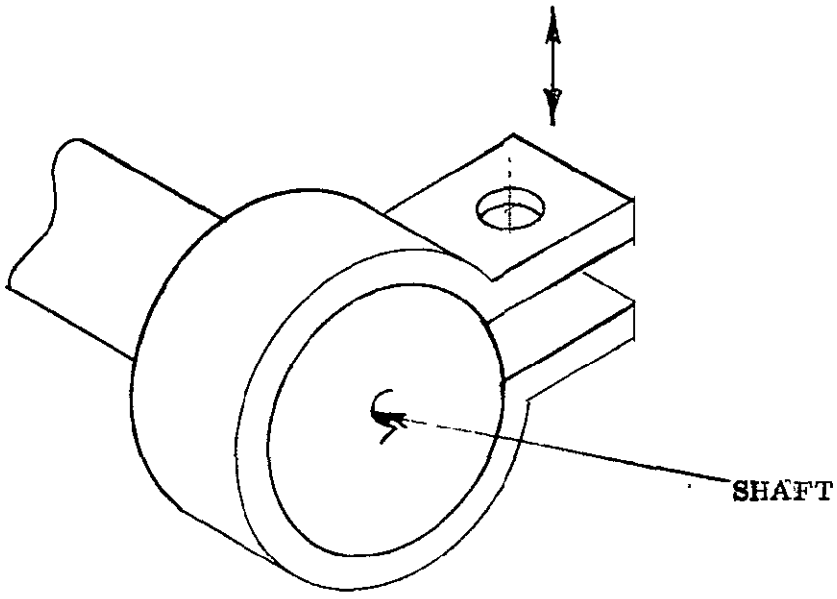

FRICTION BRAKES ON SHAFTS

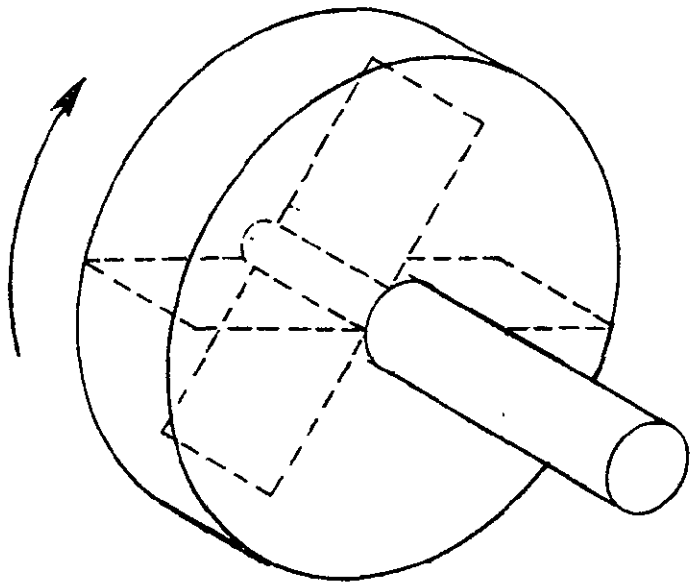

FLUID COUPLING DEVICE

FIG. 2.1.12

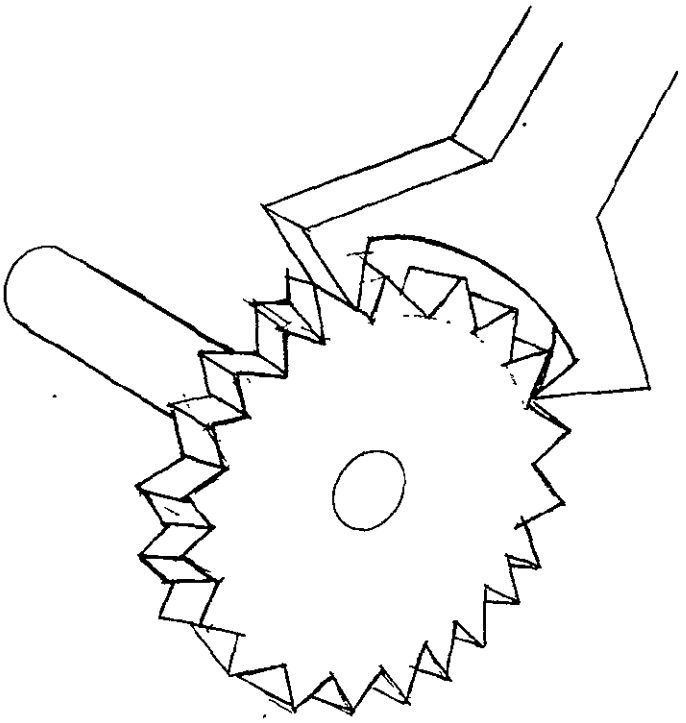

ESCAPEMENT

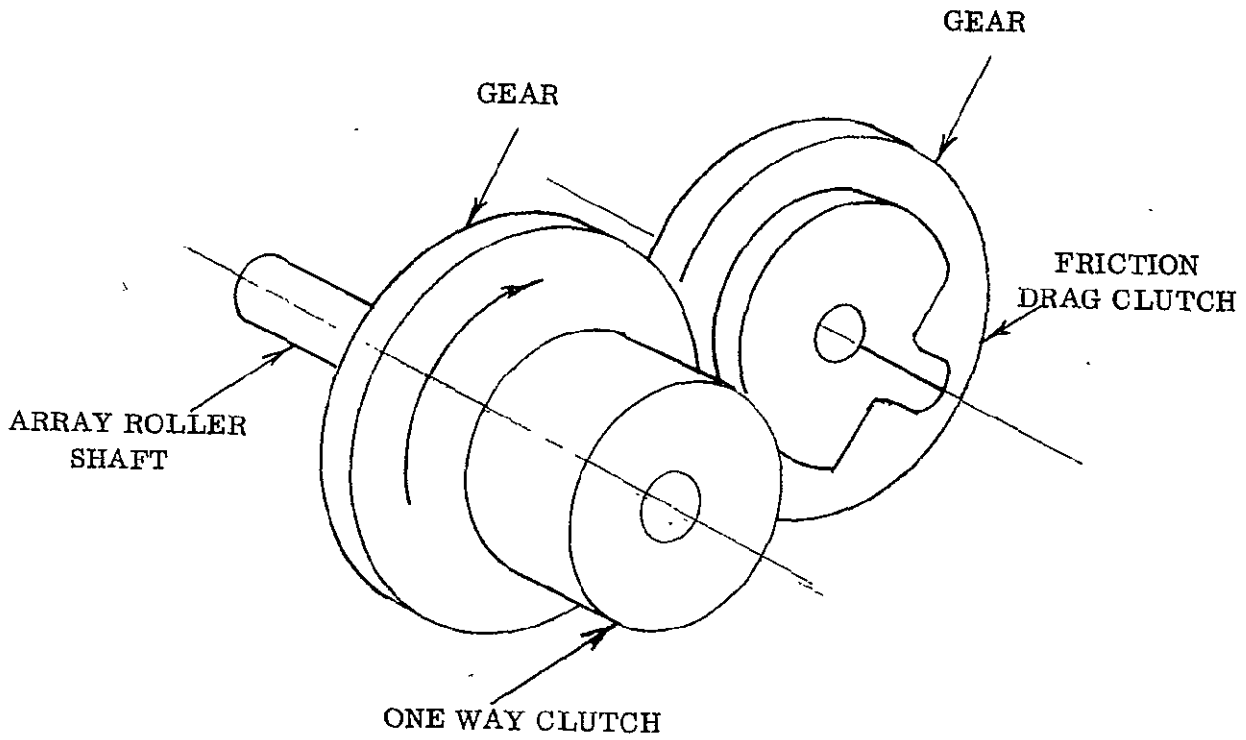

ONE WAY & DRAG CLUTCHES

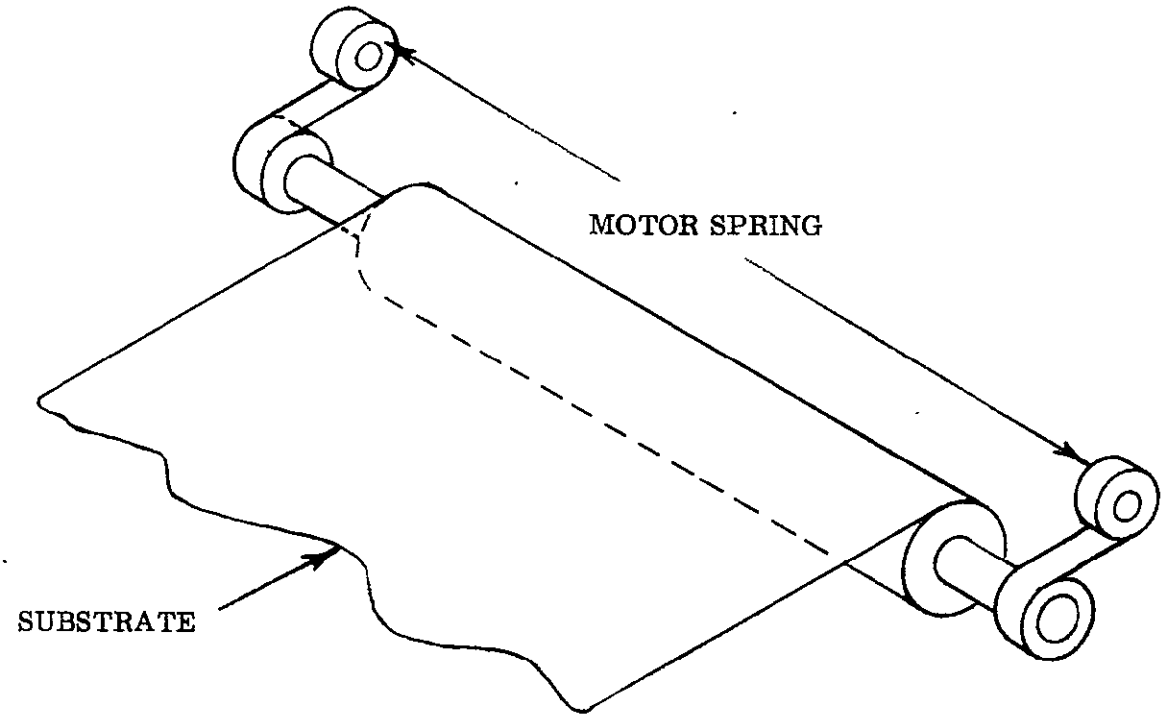

ARRAY ROLLER, WITH MOTOR SPRING TENSIONER

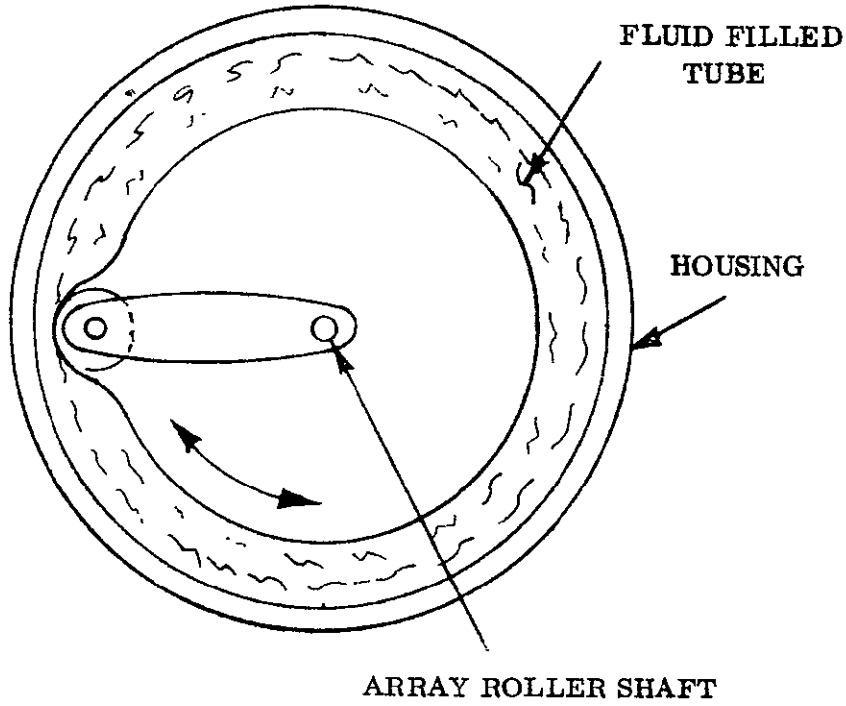

FLUID COUPLING DEVICE

FIG. 2.1.14

2.1.5.1 Deployment Link Tensioner

The deployment links can be used as a tensioner by designing the links so that they do not open into a straight line, but form obtuse angles at their intersection. At full deployment of the substrate, the links will overdrive until a predetermined amount of substrate tension is achieved.

2.1.5.2 Substrate Roller Torsion Springs

A promising concept for applying array tension uses a torsion spring mounted within storage drum. The spring is positioned around the drum shaft with one end of the spring fixed to the storage drum; the other end is mounted to a threaded collar which mates with a screw on the drum shaft. Extension of the array causes the storage drum to rotate; the torsion spring also rotates which in turn causes the threaded collar to rotate until the travel limit is reached. Any additional extension of the array results in a windup of the torsion spring thus increasing substrate tension. An advantage of this system is that the substrate tension is not applied until the end of the deployment sequence.

2.1.5.3 Array Roller With Constant Torque Motor Springs

Constant torque motor springs may be attached to the array storage drum shaft, so that during deployment the motor spring unwinds and imparts a restraining force to the roller. The design may be varied slightly by ganging the motor springs or by using adjustable tension springs if more restraining force is required.

2.1.6 Panels

There has been no effect during this reporting period on panel design concepts. Work is beginning in this area with the emphasis being placed on designing out weight where possible.

2.2 ELECTRICAL SYSTEM DESIGN

Initial efforts on the electrical system design for this program have been limited to obtaining information on the state-of-the-art of thin (8-12 mil) silicon solar cells and preliminary studies on the power/weight ratio that can reasonable be expected with a flexible, roll-up solar array. Selection of this system will be accomplished on a system engineering basis as design restraint requirements become evident.

2.2.1 Design Parameters

Electrical design and fabrication of an efficient roll-up solar array is limited by two (2) major factors. These are:

- Electrical characteristics
- System configuration

2.2.1.1 Electrical Characteristics

An analysis of thin silicon solar cell characteristics is being performed. This analysis will cover, but will not be limited to:

- Spectral characteristics
- Efficiency (at AMO)
- Temperature deviations (vs cell efficiency)
- Ultraviolet degradation
- Solar intensity efficiency variations
- Radiation degradation based on studies of:
  a. ohm/cm base resistivity
  b. thickness of cells
  c. thickness vs. efficiency of cover glass filters
  d. thickness vs. efficiency with various shielding materials
  e. particle radiation effect

2.2.1.2 System Configuration

Concurrent with the studies outlined in section 2.2.1.1, an analysis is being performed to determine the most efficient system configuration. This analysis will

concern itself with cell installation, panel layout, and panel size. It will cover the following major areas and other parameters as their importance becomes evident:

- Bus bar routing and configuration
- Power output requirements
- Voltage output requirements
- Reliability
- Repairability
- Producibility
- Cable material (weight and power loss)
- Flexibility
- Packing factors
- Expandability
- Interference (from self-generated magnetic fields)
- Test capability

2.2.2 Magnetic Effects and Short Circuits

Any attemp to minimize magnetic effects in a deployable solar array involves a system trade-off in wiring reliability and therefore an inherent possibility of short circuits. Figures 2.2.1 and 2.2.2 illustrate module bus bar designs of a short-free or a minimum magnetic interference configuration.

2.2.2.1 Magnetic Interference Considerations

A minimum magnetic interference configuration requires an approach which will minimize the net magnetic field due to current flowing through solar cells, conductors, and bus bars. The optimum method to meet this requirement is to have equal current paths through adjacent modules and bus bars, but current flow in opposite directions. This causes the magnetic effect of any two adjacent modules to cancel each other.

In designing for a minimum magnetic configuration, however, the possibility of a short circuit is increased. Since adjacent modules contain different electrical potentials, contact between any component on the modules will result in a short circuit. In working with extremely lightweight, deployable arrays, the amount of

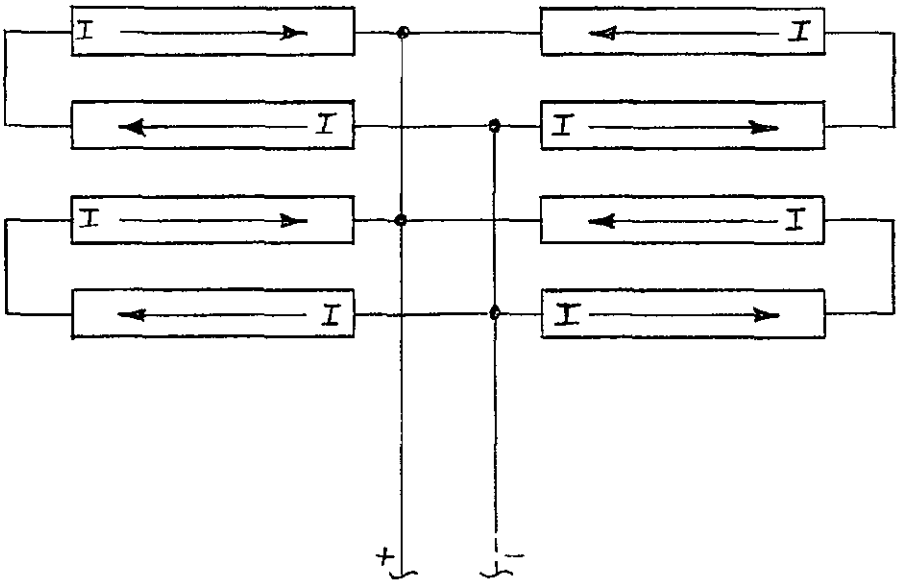

Minimum Magnetic Interference

Fig. 2.2.1

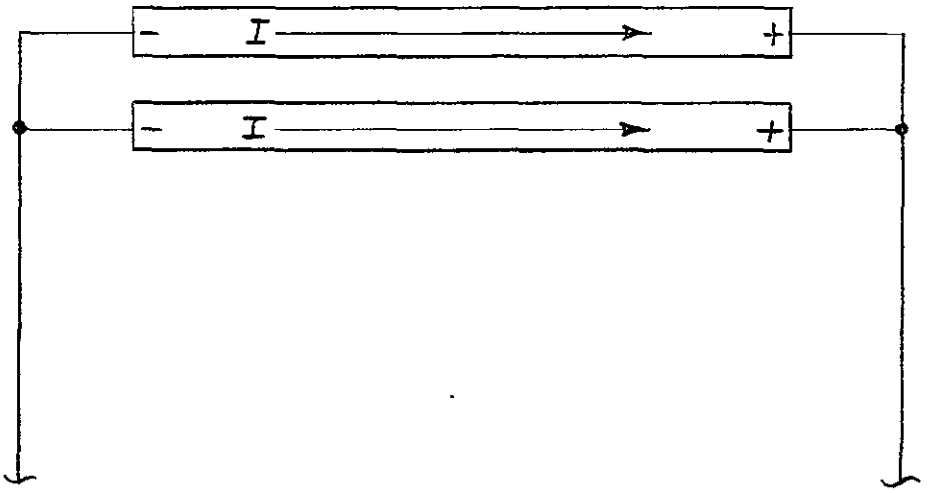

Non-Shorting Configuration

Fig. 2.2.2

insulation which is used has a direct effect upon system weight. Therefore, a minimum amount of insulation is desirable. One method of reducing insulation requirements is to arrange electrical components and circuits so that the potential difference between adjacent circuits and components is minimized. The probability of contact between adjacent electrical circuits is increased in a flexible array because of the relative motion induced in components during extension or retraction. Short circuits can arise in both the fully deployed condition and during deployment. The latter condition may aggravate the problem, since during deployment part of the array will be illuminated and the remainder will be shielded from the sun giving rise to large potential gradients between adjacent circuits. Possible weak points are under more stress in the rolled section and a short can occur more easily resulting in damage and possibly even welding together of the shorted elements. Through the use of suitably located disconnect diodes, it is possible to prevent the entire array from being disabled due to shorts. It should be pointed out that a minimum magnetic configuration for a deployable array requires more area and therefore incurs a weight per watt output penalty.

2.2.2.2 Electrical Potential Isolation Considerations

A configuration which exhibits the greatest potential of freedom from shorting is presented in Figure 2.2.2. A disadvantage of this configuration is that it probably will generate relatively large magnetic fields With this approach, possible electrical shorting paths are virtually eliminated, because adjacent modules and components contain the same potential at points likely to come into contact with each other. Since there are no adjacent bus bars or crossing electrical connections, little possibility for these elements to "short" exists. Additional studies of these and other configurations will be required prior to selecting a final design.

2.3 STRUCTURAL ANALYSIS

Parametric structural studies to be used as input to the total system analysis were begun. The effort has been concentrated in two areas, namely; the solar panel and supporting structure.

2.3.1 Solar Panel Natural Frequency

The solar panel was evaluated in its deployed attitude to evaluate the minimum natural frequency requirement of 0.04 Hz. A nomogram, Figure 2.3.1, was developed for a range of panel lengths, unit weights and tensions. It demonstrates the ability of any developable configuration to readily comply with the specification. The membranous panel was treated as a string whose fundamental natural frequency is obtained from the following equation:

$$F_n = \frac{1}{2L}\sqrt{\frac{T}{\gamma}}$$

T = Tension per foot of width, lb.

γ = Mass per square foot

L = Length, ft (Active plus 4.5 for shadow loss)

It should be noted that the frequency is independent of material elastic properties.

The most promising deployment structures are the folding arm, the Tubular Extendible Element (TEE) and the collapsing tube. These concepts are being investigated for the following materials:

- Aluminum
- Steel
- Titanium
- Beryllium
- Beryllium copper
- High modulus, metallic fiber reinforced plastic composite

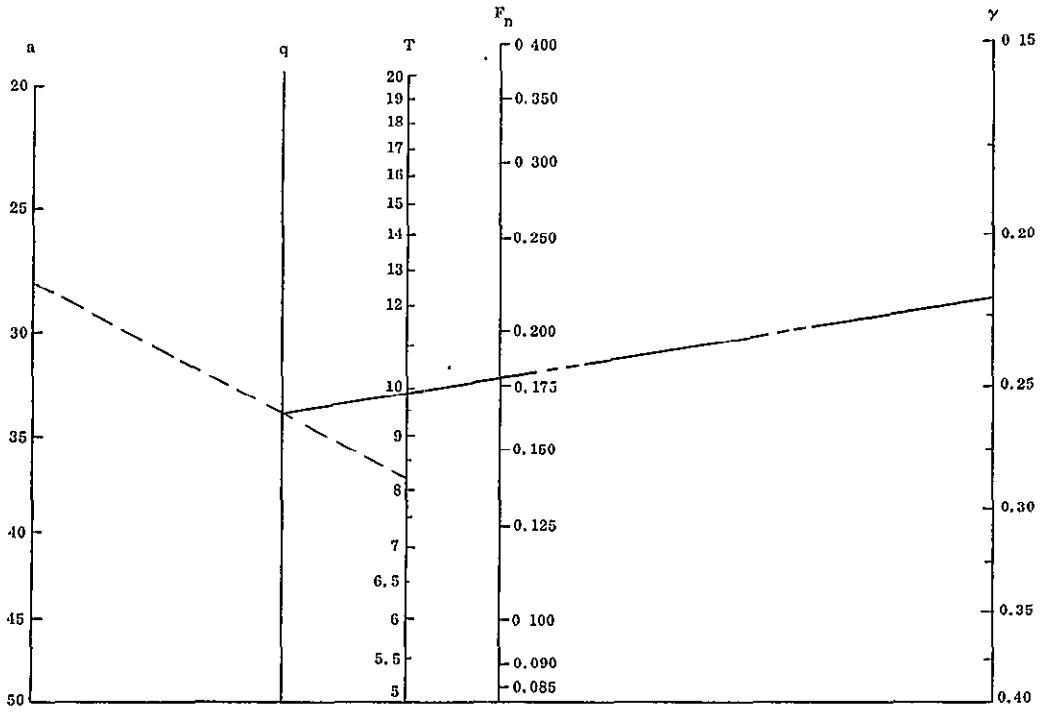

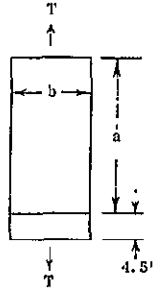

$$F_n = \frac{1}{2(a+4.5)}\sqrt{\frac{T}{b}\cdot\frac{g}{\gamma}}$$

a = Length of Array Covered by Cells, (FT)

b = Panel Width (FT)

$a \times b = 250\ ft^2$

T = Total Tension Load (LBS)

γ = WEIGHT OF SUBSTRATE & CELL STACK (LB/FT^2)

$g = 32.2\ FT/SEC^2$

F_n = Natural Freq. of Substrate (Hz)

(Design Includes 4.5 ft of extra length of substrate due to shadow line compensation)

Figure 2.3 1

SOLAR PANEL SUBSTRATE NATURAL FREQUENCY AS FUNCTIONS OF PANEL GEOMETRY, MASS, & SUBSTRATE TENSION

2.3.2 Collapsing Tube

A limited preliminary analysis has been conducted on the collapsing tube design. Steel, titanium and beryllium copper have been evaluated. Beryllium copper was included in the initial group due to FHC's extensive experience using the metal in extendible tubular boom designs for use in similar applications. Beryllium and beryllium wire and boron filament materials will be evaluated although their use for this concept is problematical. The use of either is an extension of the state-of-the-art.

Typical forseeable problems are:

- Notch sensitivity of beryllium and its effect on the tabs and slits.
- Boron filament memeber required metal edges configured to the locking device to be bonded to the basic tube material.
- Internal loads generated by differences in coefficients of thermal expansion between tube material and edge interlock material.

Analyses of 3 materials to date (titanium, steel, and beryllium copper) indicate a titanium tube to be the lightest (Ref Table 2.3.1). The tube is analyzed as a cantilever beam column subjected to an axial end load and moment. The moment is caused by the eccentricity of the solar panel plane with the tube center line. More refined analyses at a later date will consider the shear effect at the end of the tube if angularity exists between the solar panel and tube. This will be developed during the design evolution. Constants assumed for the first run analysis are:

- Tube diameter = 5 in.
- Minimum wall thickness = 0.002 in.
- Tube length = 25 ft.
- Eccentricity = 9 in.

Material	Substrate Tension		
	10 lb	15 lb.	20 lb.
Titanium	1.89	2.19	2.64
Steel	2.67	3.23	3.70
Beryl-copper	3.55	4.19	4.91

Table 2.3.1

Weight of 25 Foot Collapsing Tube

The methods of analysis used to obtain the above designs are:

Beam Column Equations

$$M_{max} = \frac{M_1}{\cos \frac{L}{2j}}$$

$$\delta_{max} = \frac{M_1}{P} \left(\frac{1 - \cos \frac{L}{2j}}{\cos \frac{L}{2j}} \right)$$

where $\frac{L}{2}$ = cantilever length = 25 ft.

Allowable Stresses

$$F_c = \frac{\pi^2 E}{\left(\frac{L}{\rho}\right)^2}$$ Euler's equation

$$\sigma_{cr_c} = \eta \frac{CEt}{R}$$ for axial compression, Ref. NACA TN3783

$$\sigma_{cr_b} = 1.3 \, \sigma_{cr_c}$$ for bending Ref. NACA TN D-163

$$M.S. = \frac{1}{R_c + R_b} - 1$$

2.3.3 Folding Arm

Parametric studies were initiated for the folding arm concept. Ranges for the variables are:

1. Solar panel width - 6 to 12 ft.
2. Arm segment length
   a. Group A - Arms as long as possible with a maximum of 14 ft.
   b. Group B - Arm length equal to solar panel width.

   The comparison in number of arm segments for Groups A and B is shown in Figure 2.3.2.
3. Solar panel substrate tension - 5 to 20 lb.
4. Materials - Aluminum, titanium, beryllium and boron filament laminate.
5. Actuating Mechanisms
   a. Cable Sprocket - critical as a beam column due to cable pre-load.
   b. Torque Tube - critical in torsion

   A thin-walled square tube will be used as it is most adaptable for mechanism installation and has high structural efficiency which can be further enhanced by corrugating the faces.

2.3.4 Preliminary Analyses of a Typical Folding Arm Design

The following thread-line case is presented to illustrate the methods of analysis being used in the study. Results will be presented in later reports.

Natural Frequency Analysis

Stiffnesses necessary to meet the 0.04 Hz. minimum natural frequency requirement in bending and torsional modes are determined.

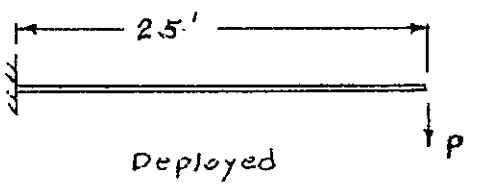

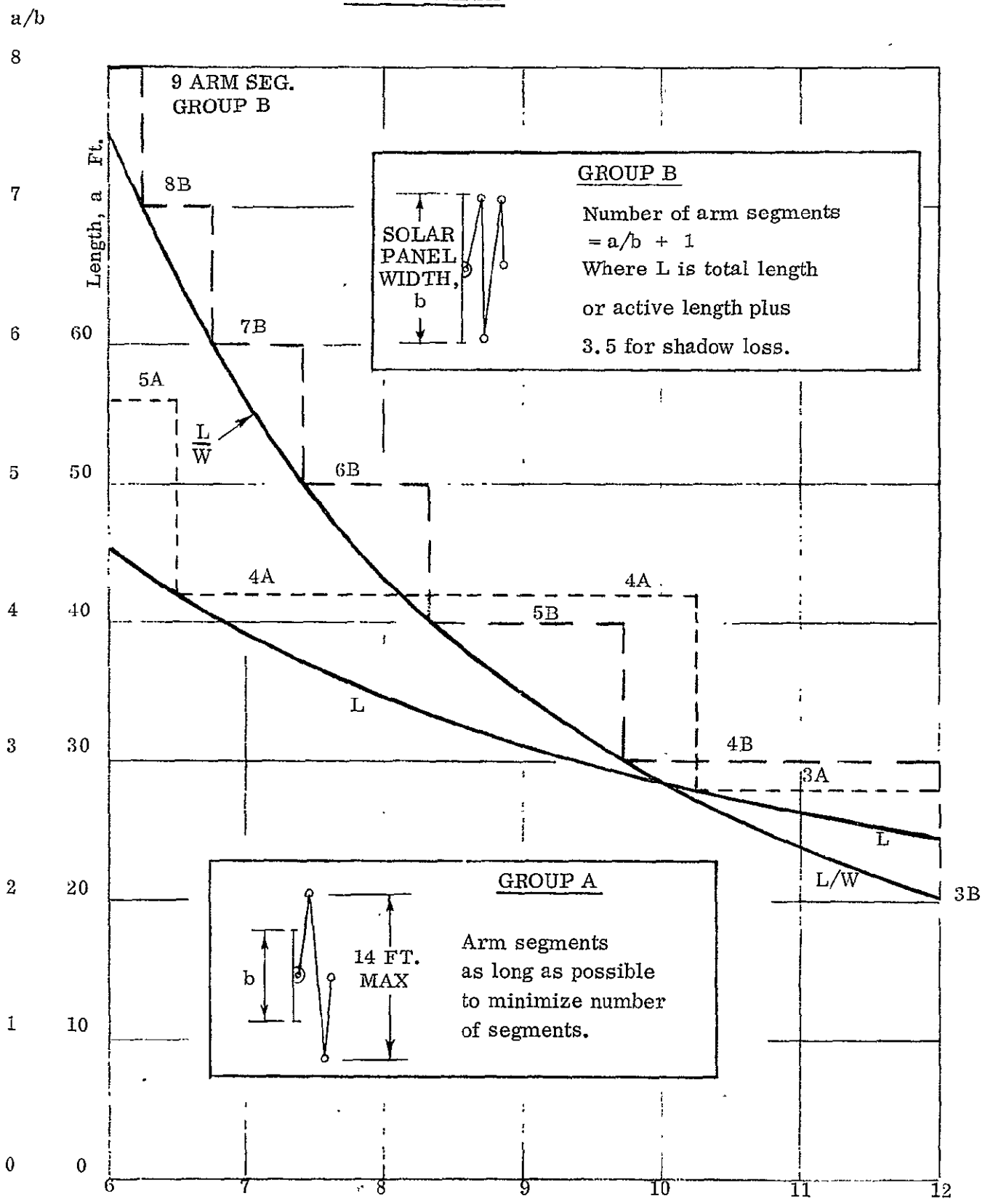

FIGURE 2.3.2

FOLDING ARM-GEOMETRIC DATA

Bending

P_A = 0.5 x solar panel wt. = 0.5 (50) = 25# concentrated at tip

Beam + deploy. mech. (P_B) = 15# distributed

The distributed mass can be represented by locating 23% of it at the tip as concentrated.

$$P = P_A + .23\, P_B = 28.5\#$$

$$m = 28.5/386 = .075$$

$$f_n = \sqrt{\frac{3\ EI}{L^3 m}} \Big/ 2\pi$$

Setting f_n equal to 0.04, per requirement:

$$EI_{REQ.} = \frac{4\pi^2 f_n^2 L^3 m}{3} = \frac{4\pi^2 (.04)^2 (300)^3 (.075)}{3}$$

$$= 42500$$

Required EI is below that of any practical size tube and indicates 0.04 Hz to be no problem. The coupling effect of the natural frequencies of the solar panel and the supporting structure will be evaluated during later phases of the study.

Torsional Natural Frequency

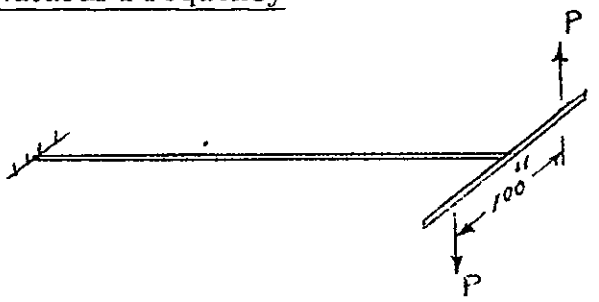

$P = .25\ (50) = 12.5\#$

$m = 12.5/386 = .0324$

$$f_n = \frac{1}{2\pi}\sqrt{\frac{K_t}{I}}$$

where

K_t = Torsional shaft stiffness, lb. in/rad

I = Mass moment of inertia of end mass, lb. in-sec^2

I = $2\,(50)^2\,(.0324) = 162$

Assuming a square cross-section:

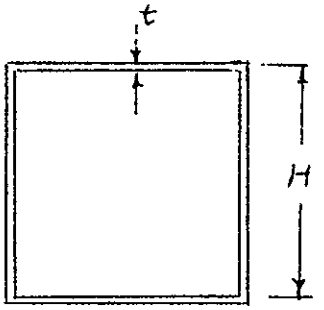

$$K_t = \frac{GJ}{L} \quad \text{where } J = \frac{4A^2}{\oint \frac{dh}{t}} = \frac{A^2 t}{h} = h^3 t$$

For a 1" square box:

$$K_t = \frac{G\,(1)^3 t}{(300)} = .00333\ Gt$$

$$f_n = \frac{1}{2\pi}\ \frac{.00333Gt}{I} = \frac{1}{2\pi}\ \frac{.00333Gt}{162} = .000728\ Gt$$

Setting f_n at 0.04, Required Gt = 3020

Any practical thickness will more than satisfy the requirement.

Orbital Angular Acceleration Forces

The array shall be designed to withstand a maximum amplitude of 2×10^{-5} radians/sec^2 pitch angle acceleration in the deployed configuration. Reference Para. 3.9.3 of the JPL Specification.

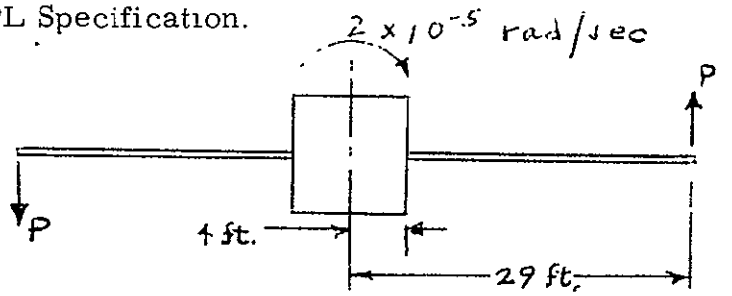

One half of each 50 pound solar panel will be applied to the tip of the supporting structure

$$P = MR\alpha = \frac{50}{2 \times 32.2} (29)(2 \times 10^{-5}) = .45 \times 10^{-3} \text{ lb.}$$

The load is small enough to have no significant influence on the column allowable required to support the solar panel preload.

Strength Analysis

The required wall thickness of a 4 inch square beryllium tubular arm is determined for a 20 pound solar panel end load. The analysis is for a configuration with arms containing an internal sprocket-cable deployment system.

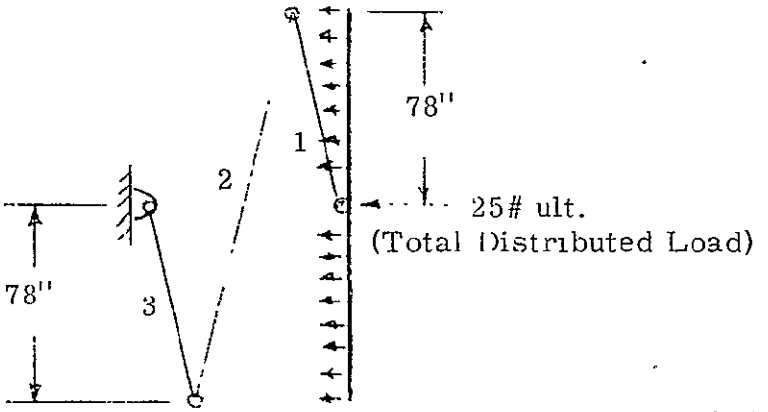

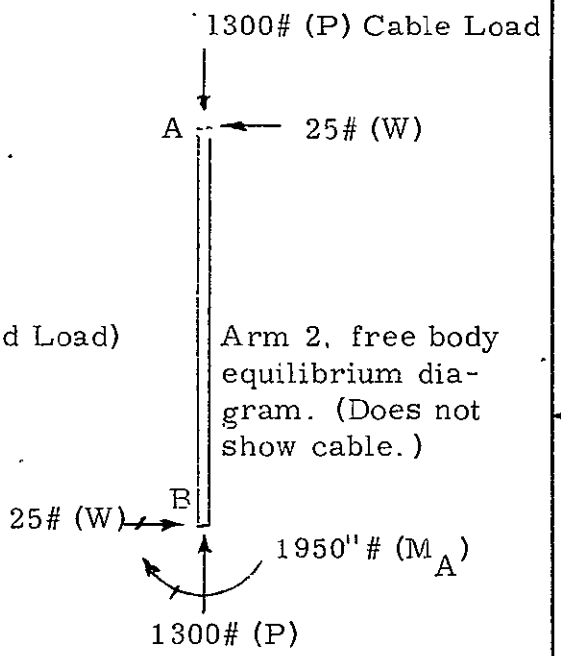

Sprocket radius = 1.5"

$M_A = 25 (78)$ = 1950"#

Column load = 1950/1.5 = 1300# (and cable load)

The arm is analyzed as a cantilevered beam column.

$$\text{Max. } M = - W_J \tan\left(\frac{L}{j}\right)$$

where $$J = \sqrt{\frac{EI}{P}}$$

$E = 40 \times 10^6$ psi

The tube wall is corrugated to develop an allowable local buckling stress of 35 KSI. For the practical minimum thickness of 0.012 in., the maximum bending plus axial stress is 32800 psi.

Although the internal drive system presents a very clean design, the penalty is the restriction on the sprocket radius to less than half the arm width and the ensuing high cable and column loads. A weight optimization study is conducted on the following pages for externally mounted sprockets.

Conclusions

The derivation of the curves in Figure 2.3.3 indicated a high degree of sensitivity of required arm size as a function of applied end load from the solar panels. Obtaining an optimum design for high end loads requires a configuration falling in the proper range of the tan L/j function of the beam column equation. This will dictate the need for careful design and analysis to minimize eccentricities and stress concentrations. Straightness and thickness tolerance control in fabrication will also be important.

Figure 2.3.3 reveals that the weight of the beryllium structure is approximately one-half that of the aluminum. As stability is the designing factor, the superiority of beryllium's modulus of elasticity to density ratio yields the lighter structure. The design of the arms is considered critical for loads encountered during solar panel deployment. They can be suitably supported in the stowed configuration.

As the analysis of the typical configuration indicated, the arms are critical for column stability. The parametric study presented herein assumes the pulleys on the long intermediate arm to be externally mounted. This permits a doubling of the pulley radius resulting in a 50% reduction of the column load induced by cable tension. Preliminary analysis shows that the bending moment on the arm due to the external cable load is a small penalty to pay for the large reduction in column load. The arms were optimized for beryllium and aluminum subjected to solar panel end loads up to 40 pounds (limit). Two physical limits were established:

1. Maximum tube size = 4.5 in.
2. Minimum wall thickness = 0.012 in.

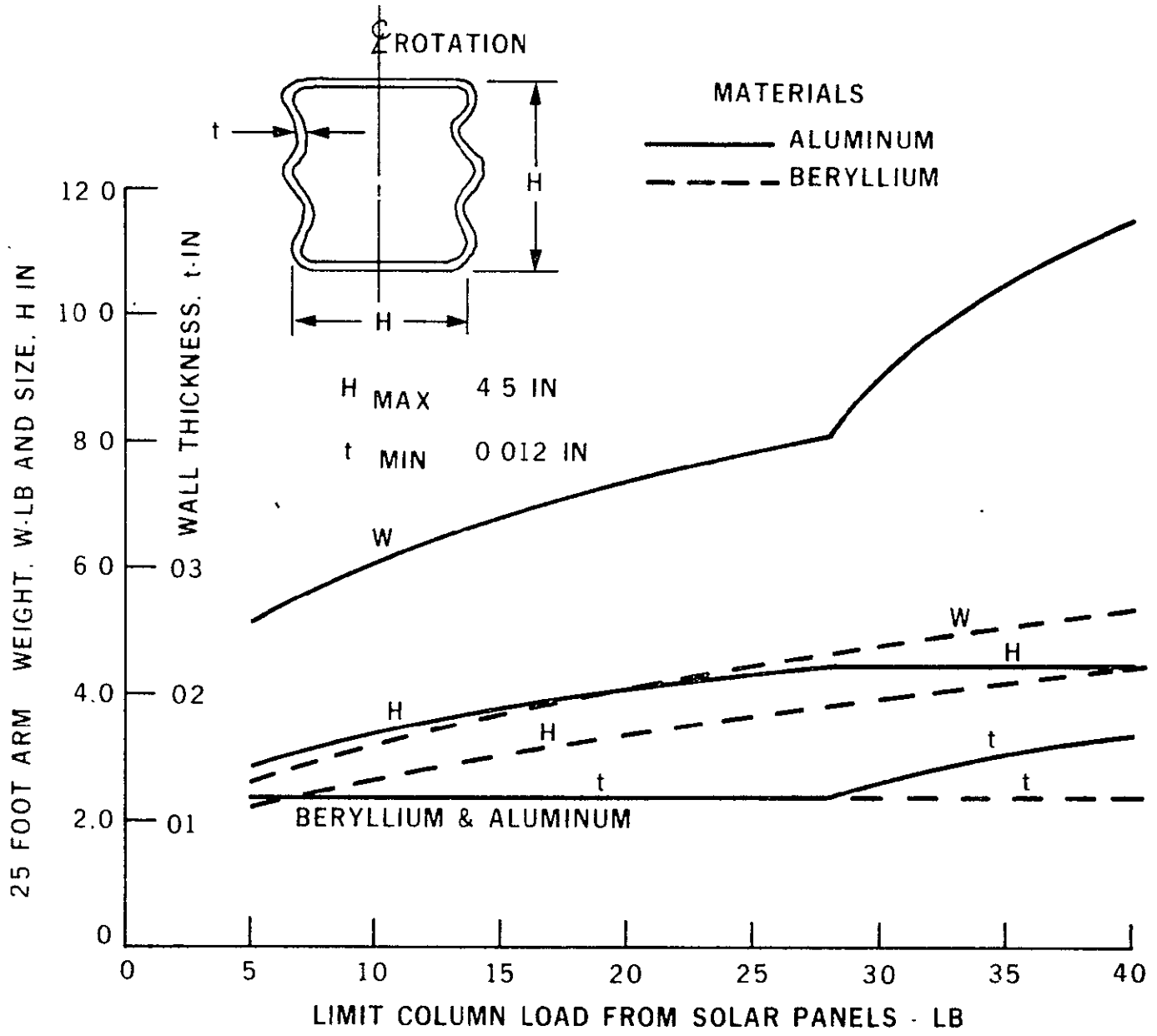

Figure 2.3.3 Folding Arm Structural Weight vs Column Load

The two side walls are corregated to develop the following local crippling allowables:

F_{CR} = 50 KSI for aluminum
F_{CR} = 35 KSI for beryllium

The upper and lower faces need not be corrugated as maximum stresses from beam bending are in the sides.

2.3.5 Preliminary Analysis of a Typical TEE Structure Design

The TEE in the deployed configuration is critical as a column for the preload applied by the solar panel. It also must comply with the minimum first mode natural frequency requirement of 0.04 Hz in accordance with the JPL Specification. Two TEE elements are used to obtain adequate torsional stiffness through differential bending of the elements. This approach is necessary since the TEE element is very weak in torsion, being an open section.

Typical Column Analysis Study

The method of analysis used here in is from Appendix B of FHC-SESD Report SSD 145.1, "A Proposal for Assembly and Maintenance of Lightweight Metallic Structures", dated November 1966. Stainless steel and beryllium copper are evaluated and presented in Figure

Allowable column load, P_{CR}, is given by

$$P_{CR} = \frac{K_C}{2} \qquad \frac{CR^3 t^3 L^2 + DR^7 t}{FR^4 L^2 + Ht^7 L^4}$$

where K_C, C, D, F and H are functions of material, overlap angle, and end fixity. P_{CR} is a linear function of Young's Modulus, E. As these variables were derived for an E of 10×10^6 psi (beryllium copper) in the FHC report, F_{CR} can be obtained for other materials by ratioing E's.

Minimum R/t of the TEE is limited by F_{cy} of the material. The tape shall be front wound as shown in the sketch to minimize principal and shear stresses.

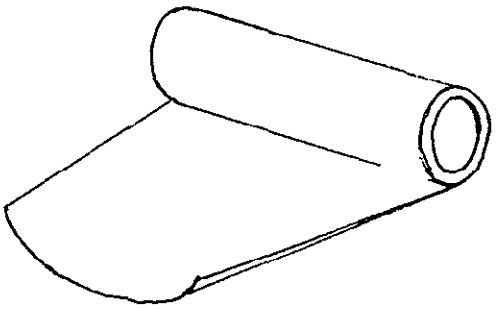

Radius of roller will be at least as large as the TEE radius.

From basic beam theory, $R = EI/M$

$$M = \frac{EI}{R} = \frac{E t^3}{12R} \quad \text{(neglecting Poisson's ratio effects)}$$

$$f_b = \frac{Et^3}{12R} \times \frac{6}{t^2} = Et/2R$$

$$R/t = E/2f_b$$

For beryllium copper:

F_{cy} = 120 KSI Work to 80% of F_{cy}

$$R/t > \frac{E}{2F_{cy}} = \frac{18 \times 10^6}{2\,(96 \times 10^3)} = 94$$

For stainless steel:

F_{cy} = 140 KSI Workup to 80% of F_{cy}

$$R/t = \frac{30 \times 10^6}{2\,(112 \times 10^3)} = 134$$

For short TEE's, two terms in the equation for P_{CR} are insignificant and the equation reduced to:

$$P_{CR} = \frac{K_c}{2} \left[\frac{D R^3 t}{F L^2}\right]$$

For a tape overlap angle of 155^{o},

$D = 8.2 \times 10^{18}$

$F = 3.1 \times 10^{10}$

$K_c = .97$

For a 25 foot (300 in.) TEE,

$P_{cr} = 179\ D^3 t$. for beryllium copper with an E of 18×10^6 psi

$P_{cr} = 298\ D^3 t$ for steel

$$\text{Tape width} = \pi D \left(\frac{360 + 155}{360}\right) = 4.5\ D$$

Tape weight assuming a 26 ft. length Wt = 41 Dt for beryllium copper or steel.

Natural Frequency Analysis

A parametric study is conducted to satisfy the requirement for the first mode natural frequency to exceed 0.04 Hz. From the referenced report in the preceeding paragraphs:

$$f_n = \frac{1}{L^2} \sqrt{\frac{36\ E\ \pi\ R^3 t}{\frac{M}{L} + \frac{.46\ \pi\ p\ R\ t\ \alpha}{g}}} \quad \text{Hz}$$

where

M = Tip mass (lb/g)

p = Wgt. density of TEE (lb/in^3)

α = Tape overlap factor = 1.43

For a 300 inch TEE and 1/4 of a 50 pound solar panel concentrated at the end of the TEE:

$$f_n = \frac{1}{(300)^2} \sqrt{\frac{113\ E\ R^3\ t}{.000108 + .00155\ Rt}}$$

The natural frequency is calculated for a 1.25 diameter TEE with 0.002 in. beryllium copper tape. This configuration was selected from Figure 2.3.4 and will have the lowest natural frequency of a TEE designed for a 5.0 pound minimum total solar panel end load

$$f_n = \frac{1}{(300)^2} \sqrt{\frac{113\,(18 \times 10^6)\,(.625)^3\,(.002)}{.000108 + .00155\,(.625)\,(.002)}}$$

$$= 1.06\ H_z$$

This easily exceeds the 0.04 minimum requirement.

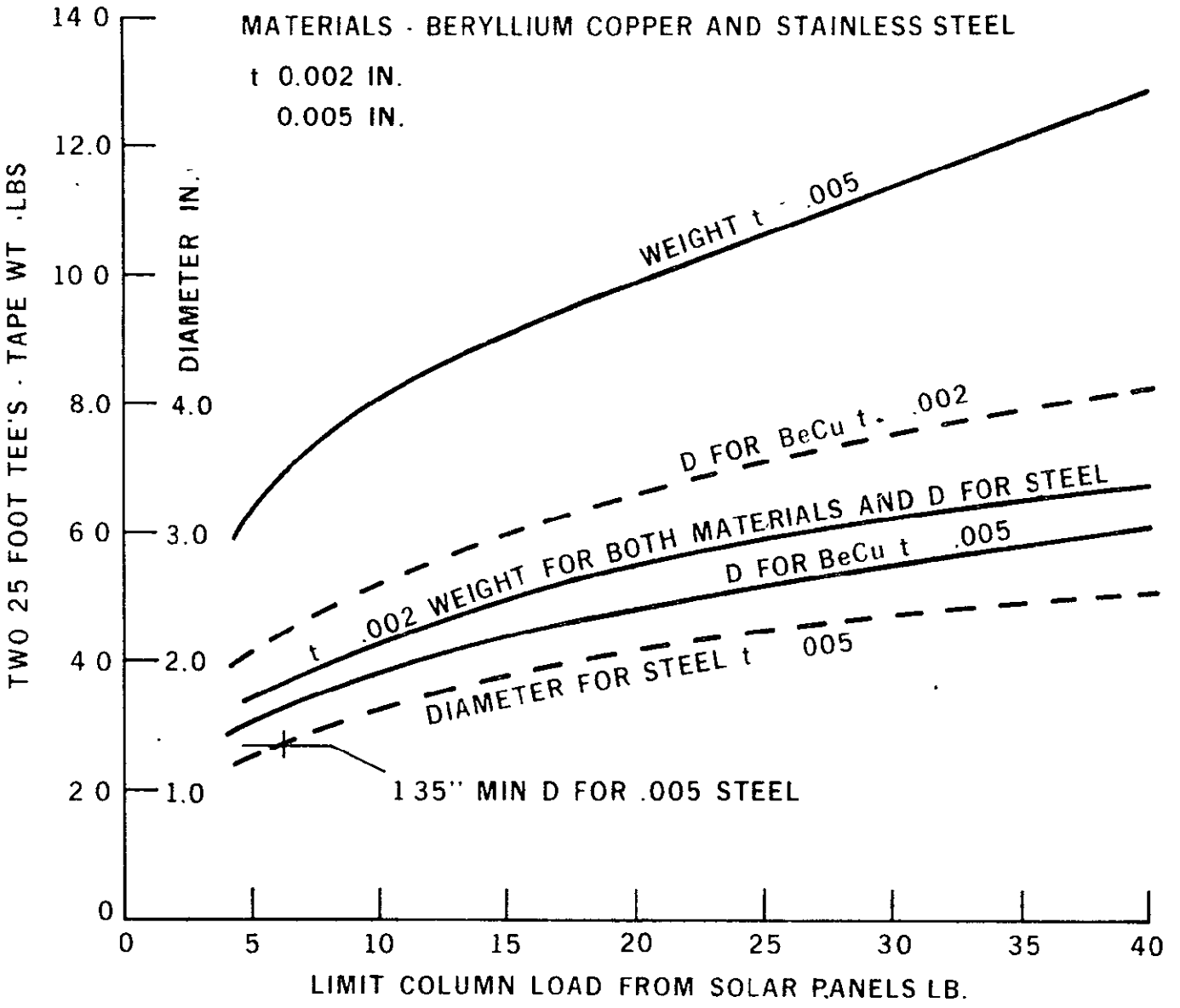

Figure 2.3.4 Weight and Size of Tubular Extendible Elements vs Column Load

2.4 MATERIALS ENGINEERING

The principal material engineering activities in this period were the review of high modulus materials, evaluation of filament reinforced materials, tabulation of room temperature properties for design analysis, tabulation of thermal control coating properties, and testing of substrate material.

2.4.1 High Modulus Materials

High modulus is required for low deflection of deployment mechanism load carrying elements. However, high modulus materials tend to low ultimate elongation, low notch tensile strength, low impact strength, and low temperature brittleness. Table 1 compares High Modulus Materials and shows that fiber reinforced laminates, beryllium, and precipitation hardening stainless steel 17-7 PH have very low (1% or less) ultimate elongations at room temperature. These materials present severe fabrication problems, as well as having a brittle nature in a low temperature application. Beryllium copper and maraging steel with elongations of 10 and 9% respectively, appear attractive because of their reasonable compromises between stiffness and toughness. Manufacturing processes for beryllium copper tubular erectable elements are currently utilized by Fairchild Hiller in the manufacture of space antenna. Preliminary evaluation of the required modification of these processes to use maraging steel in the fabrication of 4% lighter and 50% stiffer tubular erectable elements appears to be straightforward with nominal development. Higher modulus materials are being evaluated for fabrication and functional requirements, to take advantage of any significant advance in the state-of-the-art.

2.4.2 Filament Reinforced Materials

Filaments with very small diameter 1 to 3 microns (0.0004 - 0.0012 inch) have extraordinary strength approaching the atomic cohesive strength. Composite efficiency, ratio of test strength to theoretical strength, was 58% and 37% for filament wound and cross-laminated glass fiber - composite materials (13). In slender column application, the fibers should be oriented lengthwise for maximum stiffness and strength. Laboratory tests correlate theory to yield the following for multilayer glass fiber-epoxy composite (14):

- Stiffness was 7.5×10^6 psi for unidirectional (axial) fiber orienta-

tion compared to 5 x 10^{-6} psi for 30° angle orientation of crossed helical wound fiber layers.

- Ultimate tensile strength was 160,000 psi for unidirectional fibers compared to 15,000 psi for 30° winding.

Anelastic crippling probably limits the ultimate compressive strength of high modulus fiber-matrix materials. High modulus of reinforcing boron fibers allows the design of very efficient compression resistant structural elements. Yielding in a ductile matrix occurs at small fractions of the ultimate strength, so the advantage of high stress level capacity is attended by potential creep and fatigue limitations. (15)

Filament wound, unidirectional, 4 mil boron fiber (60% by vol.) reinforced epoxy NOL rings tested by the Air Force Materials Laboratory disclosed that very low strength in transverse directions is to be expected; 3,000 psi tensile, 17,000 psi compressive, and 8,500 psi flexural compared to 110,000 tensile, 164,000 compressive and 220,000 flexural psi strength in the fiber direction. Interlaminar shear strength 16,100 psi, is comparable to that of glass epoxy rings provided that the fibers are heated to 1500°F in dry nitrogen to remove a boron oxide film before winding. Cross ply laminates have very low interlaminar shear strength, approximately 2500 psi, because of stress concentration at the cross points of the large 4 mil filaments. Roll up elements must be carefully designed to avoid bending failures. For example; take up drums for 4 mil bare fiber must be larger than 2 inches in diameter. Modulus in the fiber direction is 24.4 x 10^6 psi. (16)

Diffusion bonding of sheet metals with reinforcing fibers between layers was also done for non-destructive test development. (17)

2.4.3 Room Temperature Properties

Data is summarized in Table 2, Room Temperature Properties.

2.4.4 Thermal Coatings

Candidate thermal coatings to meet potential requirements are shown in Table 3, Thermal Control Coatings.

2.4.5 Substrate Tests

An attempt was made to bond Kapton F film material (which includes 2 mil FEP teflon and 2 mil Kapton H film) to bare Kapton H film. The materials were cleaned using MEK solution and pressed together at 600° F and 200 psi for 3 minutes. The resulting bond had no practical resistance to peeling loads and thus is unacceptable. Therefore, several adhesive systems were evaluated. Silicone rubber adhesive A-1000 (Dow Corning) gave 36.8 - 47.2 lb/in peel strength in a bonded loop test and failed in the adhesive. Permacel 18 (Permacel Corp., New Brunswick, N. J.) solvent activated and pressure bonded at 340°F gave the highest bond strength 68-86 lb/in and failed in the 5 mil thick Kapton H substrate strips.

The results of room temperature creep tests are shown in Figure 1, Creep Data for 3 mil Kapton H Film.

TABLE 2.4.1

HIGH MODULUS MATERIALS

Material	Modulus psi	Strength psi	Density lb in $^{-3}$	Poisson Ratio	Notes
"Borofil" (1) (4 mil diameter)	60×10^6	250,000	0.095	0.04	$\alpha = 2.7 \times 10^{-6} {}^{o}F^{-1}$ (80-600°F)
Glass Fibers	7 (2)	204,000(2)	0.092(2)	0.2(3)	$\alpha = 1.8 \times 10^{-6} {}^{o}F^{-1}$ (32 - 518°F)
Borofil/Epoxy (28% Resin)	35(1)	247,000(1)	0.075(4)	0.3(est)	$\alpha = 2.7 \times 10^{-6} {}^{o}F^{-1}$ (80-600°F) $\epsilon = 0.7\%$
Glass/Epoxy (5) (35% Resin)	5	--	0.065	0.3	$\alpha = 2\text{-}6 \times 10^{6} {}^{o}F^{-1}$
Beryllium (6)	42.5	26,000	0.067	0.1	$\alpha = 6.4 \times 10^{-6} {}^{o}F^{-1}$ $\epsilon = 1.0\%$
17-7PH S.S.(7) Cond. CH900	29	255,000	0.277	0.28	$\alpha = 6.4 \times 10^{-6} {}^{o}F^{-1}$ $\epsilon = 1\%$
Beryllium Copper (8) Alloy 25, Special Age	19	165,000	0.300	0.3(est)	$\alpha = 9.4 \times 10^{-6} {}^{o}F^{-1}$ (70-600°F) $\epsilon = 10\%$
Maraging Steel (9) 18 N;200, Aged	26.2	245,000	0.289	0.26	$\alpha = 5.6 \times 10^{-6} {}^{o}F^{-1}$ (75 - 900°F) $\epsilon = 9\%$

TABLE 2.4.2 (a)

ROOM TEMPERATURE PROPERTIES

Material	Aluminum 7075 T 6	Beryllium 2% Be 0	Beryllium-Copper Alloy 25	Borofil/ Epoxy	Glass Epoxy	Kapton H
Reference Specifications	(6) (7) QQ-A-200/11 Extraded Shapes	(6) AMS-7911 Shapes	(6) (8) QQ-C-533 Strip	(1)(4) --	(5) --	(10) --
Properties						
Mech Prop.						
Ftu, ksi	76	40	160	55	80	25
Tty, ksi	65	27	120			
Fcy, ksi	67	27	120			
Fsu, ksi	46	33	87			
E, 10^6 psi	10.3	42.5	18.5	35	5	0.43
Ec, 10^6 psi	10.5	42.5				
G, 10^6 psi	3.9	20		28		
μ	0.33	(0.06)	0.3	(0.3)	(0.3)	(0.5)
e, %	7	1	1.0	0.07	2	70
Phys. Prop.						
W, lb in^{-3}	0.101	0.067	0.297	0.095	0.065	0.051
C, btu. $lb.^{-1} {}^{o}F^{-1}$	0.23	0.445	0.1	(0.23)	0,23	0.26
K, btu. $hr^{-1} ft^{-1} {}^{o}F^{-1}$	75.1	104	61	(0.16)	0.16	0.094
α, $10^{-6} {}^{o}F^{-1}$	13.1	6.4	9.2	2.7	4	11

TABLE 2.4.2.(b)

ROOM TEMPERATURE PROPERTIES

Material	Copper OFHC HARD	Silver	Stainless Steel 17-7 PH Cond. CH900	Maraging Steel 18Ni200	Magnesium AZ31B	Titanium Ti13V11Cr 3Al Aged
Reference	(11)	(11)	(12)	(9)	(6)	(6)
Specifications	--	---	MIL-S-25043 (Strip)	--	QQ-M-44 (Sheet) WW-T-825 (Tubes)	MIL-T-9046 Type IV (Strip)
Properties						
Mech. Prop.						
Ftu, ksi	64	18.2	265	195	32	170
Fty, ksi	30	7.9	250	190	18	160
Fcy, ksi					12	162
Fsu, ksi					17	105
E, 10^6 psi	17	10	29.0	26.2	6.5	15.5
Ec, 10^6 psi					6.5	
G, 10^6 psi					2.4	
μ	0.33	0.37	(0.25)	0.26	0.35	
e, %	1.5	48	2	9	12	4
Phys. Prop.						
W, lb in^{-3}	0.321	0.376	0.277	0.289	0.0639	0.174
C, btu lb^{-1} $^oF^{-1}$	0.092	0.056	(0.11)	(0.11)	0.25	0.128
K, btu.hr^{-1} ft^{-1} $^oF^{-1}$	226	242	9.5	11.3	56	4.0
α, 10^{-6} $^oF^{-1}$	9.3	9.4	6.1	5.6	14	4.8

TABLE 2.4.3

THERMAL CONTROL COATINGS

Material		α/ϵ	α	ϵ
ZnO-Silicate	Z-93	0.17	0.16	0.95
ZnO-Silicone	S-13	0.23	0.22	0.96
White Epoxy	SA 9185	0.24	0.22	0.91
White Silicone	517-W-1	0.28	0.25	0.90
White Acrylic	M49WC17	0.33	0.28	0.89
410 Steel	Sandblasted	0.88	0.75	0.85
A1-Silicone	172-A-1	0.89	0.25	0.28
Silicone	171-A-152	0.92	0.22	0.24
Black Silicone	517-B-2	1.01	0.89	0.88
Black Acrylic	M49BC12	1.06	0.93	0.88
	L6X96Z	1.11	0.93	0.84
Platinum Black		1.11	0.94	0.85
DOW-17		1.11	0.78	0.70
2024 Aluminum	Sandblasted	2.0	0.42	0.21
6061 Aluminum	Chem. Clean.	2.7	0.16	0.06
6061 Aluminum	Sanded	2.7	0.16	0.06
6061 Aluminum	Forging, Chem. Cl.	3.2	0.29	0.09
2024 Aluminum	Sanded	3.7	0.20	0.06
Inconel X	Foil	4.4	0.66	0.15
Beryllium, QMV	Chem. Polished	5.0	0.50	0.10
Gold	Hanovia 6518	6.0	0.53	0.09
Aluminum	Foil, Shiny	6.3	0.19	0.3
Aluminum	Foil, Dull	5.0	0.20	0.4

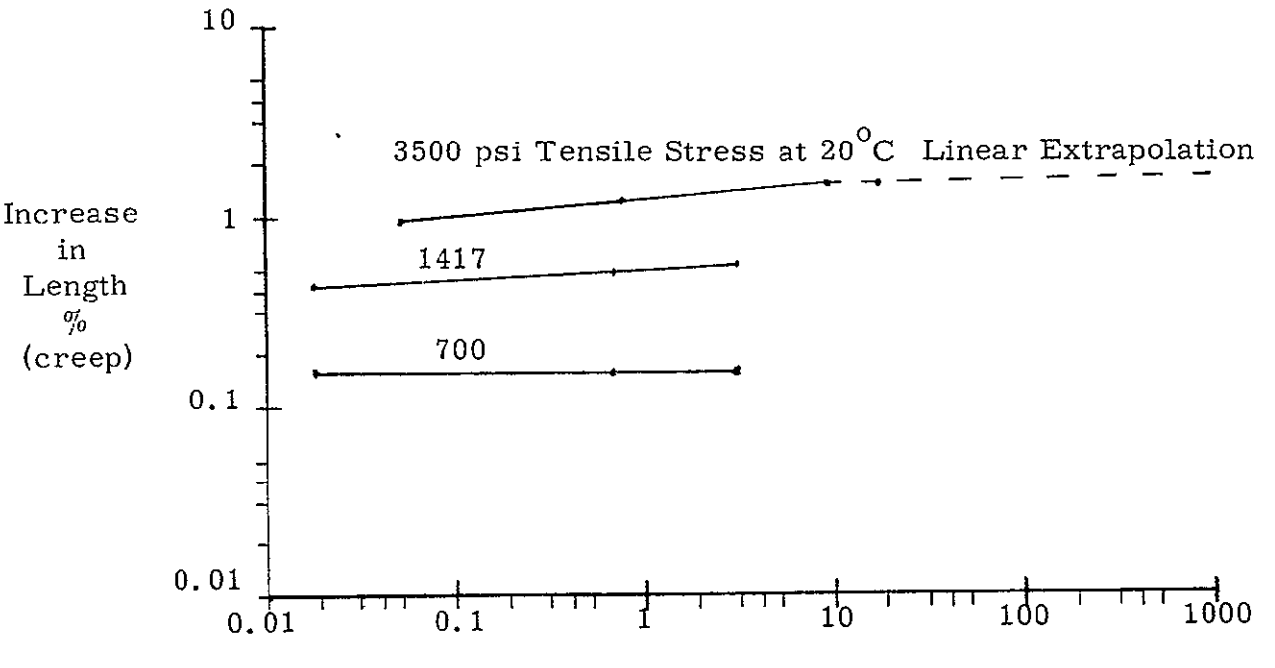

Creep Data for 3 mil Kapton H Film

Figure 2.4.1

2.5 THERMAL ANALYSIS

2.5.1 Array Front Face Thermal Control

In an effort to achieve an optimum design with respect to maximum power output per unit weight, the initial phases of the thermal study will concentrate on various means to reduce cell temperature while weighing the price, primarily in terms of weight, that must be paid to achieve these temperature reductions.

Cell temperature is basically a function of the thermal properties of all array external surfaces and the effective thermal paths between the cells and these surfaces. The external surfaces can be subdivided into five areas: (1) the cell coverglass (with respect to thermal emittance and the portions of solar energy reflected and absorbed), (2) the front cell surface (with respect to the solar energy absorbed from that which the coverglass has transmitted), (3) the exposed inter-cell wiring, (4) the interstitial area between cells, and (5) the anti-sun surface of the substrate.

The first two surfaces have not received extensive thermal examination up to this time since there is very little that can be done thermally with the limited choice of candidate cells and coverglasses. The selection of an optimum coverglass which reflects a maximum of the solar energy which the cell is not able to utilize and transmits, with minimum absorptance loss, that portion of the solar spectrum which the cell can use, is well defined and straightforward. A 3 mil glass differs negligibly in thermal emittance from thicker glasses, so there are no thermal considerations in thickness selection unless candidate coverglasses become much thinner.

The remaining external areas of concern must each be examined with respect to the means of reducing cell temperature. Ideally, the area between cells should have a solar absorptance of zero and unity emittance. This is especially pertinent to the exposed wire area, since the metallic wire offers a relatively good thermal path from cell to space sink. The wire itself is a poor candidate for an external surface. Although it is of relatively low absorptance, its emittance is even lower, and the net effect is a rise in cell temperatures. To determine if an appropriate thermal coating over this wire is worthwhile, the temperature difference between the uncoated and coated wire configurations must first be evaluated.

Assume that 10% of array front surface is area between cells and subject to thermal coatings. Of this, at most half is exposed wiring, or 5% of total frontal area. To determine an upper limit on the difference between average cell temperature with and without wire thermal coatings, consider the bare wire as $\alpha = .4$, $\epsilon = 0$ and the modified wire surface as $\alpha = .4$ and $\epsilon = .85$. Assuming an isothermal cell assembly, a one Solar Constant input, and all other thermal parameters equal, cell temperatures will differ by some $3.5^{\circ}F$, implying a difference of approximately 1% in power output.

To reduce the solar absorptance of the interstice volume between cells (the remaining 5% of frontal area), there must be a minimum of concavity so as to minimize the tendency to trap, through multiple reflections, any incident solar energy. This will cost in weight of filler material (most likely cell-to-substrate adhesive) and an increased demand upon quality fabrication to insure a smooth surface. Is it worthwhile to fill this volume between cells so as to reduce absorptance? Assume the emittance of the unfilled and filled volumes to be equal (actually, the cavity configuration will offer a slightly higher emittance) and the absorptance of the unfilled and filled cavities to be .9 and .4 respectively. The area in question being 5% of the total frontal area, and all other thermal properties remaining constant, the difference in (isothermal) cell assembly temperature would be $5^{\circ}F$, or a power difference of some 1-1/2%.

Therefore, the most that could be expected by modifying the entire 10% of the frontal area available for thermal coatings is approximately a 2-1/2% increase in power output due to a $8.5^{\circ}F$ temperature reduction. It should be emphasized that this 2-1/2% increase is definitely an upper limit, since the difference in thermal properties between the treated and untreated areas was taken to be a maximum, and, most importantly, the assumption of an isothermal cell assembly is imperfect due to far from perfect lateral conductance. Cell temperature will be primarily influenced by the thermal properties of the coverglass and the cell itself, and, where cell and non-cell frontal areas differ in thermal properties, there will be a temperature gradient from the cell center to its edges, with a definite temperature difference between the average cell and the average interstice temperature. A detailed

analytical thermal model, consisting of a representative section of the entire array assembly divided into a sufficient number of isothermal nodes, will be developed later in the program to determine this exact temperature profile. This thermal model will be developed as an analytical evaluation aid for all candidate array designs, even though it may soon be determined that the additional weight in fillers and coatings necessary to gain this aforementioned maximum of 2-1/2% power increase is too high a penalty to pay.

Since cell output increases with decreasing temperature, the question naturally arises: Why not substitute for some front surface area, formerly devoted to cell area, a surface of low solar absorptance and high emittance which, if thermally well coupled to the cells, would cause a temperature drop sufficient for an overall increase in power-to-weight ratio? In response to this question, power output as a function of solar flux, including temperature effects, will be determined.

For a unit area, the temperature of the isothermal array is expressed in the relation

$S \alpha = \sigma \epsilon_{eff} T^4$, where S is the incident solar flux.

Differentrating with respect to S,

$$\frac{dT}{T} = \frac{1}{4} \frac{dS}{S}, \text{ or for small changes,}$$

$$\frac{\Delta T}{T} = \frac{1}{4} \frac{\Delta S}{S}.$$

Assuming a solar cell output proportional to incident solar intensity S, then

$$\frac{dP}{P} = \frac{dS}{S}, \quad \text{or} \quad \frac{\Delta P}{P} = \frac{\Delta S}{S}$$

A reasonable estimate of power degradation with respect to temperature is a linear 1/2% / ^{o}K, or

$$\frac{dP}{P} = -.005\,dT, \text{ or, again for small changes,}$$

$$\frac{\Delta P}{P} = -.005\,\Delta T$$

Therefore $\left.\frac{\Delta P}{P}\right|_{total} = \frac{\Delta S}{S} - .005\left(\frac{1}{4}\ T\ \frac{\Delta S}{S}\right)$

or $\left.\frac{\Delta P}{P}\right|_{total} = \frac{\Delta S}{S}\ (1 - .00125\ T),\quad T \text{ in } {}^{o}K$

With T in the neighborhood of $320^{o}K$,

$$\frac{\Delta P}{P} = +0.6\ \frac{\Delta S}{S}\ .$$

Thus it is seen that the change in cell power output with respect to solar intensity change is positive, or an increase in intensity will result in a power increase despite the adverse temperature effects. This basic conclusion is, of course, intuitively obvious; the rate of increase (i.e., the 60% proportionality factor in the last equation) is not.

Now assume for the area to be used for temperature reduction an absorptance of zero and an emittance equal to that of the cells. Thus the absorbed solar flux per unit area (for both power and temperature considerations) is directly proportional to the fraction of the total area that is solar cell. Further, assume that the density of this hypothetical solar cell array, including the "thermal control areas" is constant per unit area. This is not an unreasonable assumption, since in order for these areas to be effective, conductance through them in the lateral direction must be appreciable, implying a relatively heavy metallic conductor. Thus the effect of assigning, say A% of the total frontal area of the panel to "thermal area" will be to effectively reduce the total solar flux S by A%. The array will therefore run cooler, weigh the same, but produce less power.

Apparently this scheme must be abandoned unless the unit weight of the "thermal area" were somehow made substantially less than the unit area weight of the solar cells while still maintaining worthwhile lateral conductance and surface emittance and near zero absorptance. Indeed, in the extreme limit of a virtually weightless "thermal area", any tendency for this area to run cooler than the cells would benefit array power output. Then consideration must of course be given the resultant decrease in power/unit area output of the array, an undesirable trend. Needless to say, this design concept is, at present, rife with practical obstacles and

is primarily of academic interest.

The preceeding relationship expressing power change with incident solar flux also indicates that any additional solar energy, such as Earth albedo or uniform solar reflections from external spacecraft surfaces, will not be unwelcome despite higher temperatures. Indeed, if there were a scheme to erect a "weightless" reflecting area adjacent to the array proper (essentially creating a solar energy "collector"), the solar flux on a given cell area, and thus the power-to-weight ratio, would increase.

2.5.2 Array Back Face Thermal Control

Efforts to optimize, with respect to cell temperature, the relatively small area of the sunlit surface available for temperature control (other than the cells themselves) are seen to be somewhat futile. The most fertile area for cell temperature reduction is the anti-sun surface, (the anti-cell substrate surface), and here too, the selection of an optimum thermal design is not so straightforward. All efforts to obtain a minimum resistance path (i.e., a maximum effective emittance, ϵ_{eff}) from cell to space must be weighed against the attendant cost in weight and complexity.

The initial thermal design effort (presently underway) is attempting to determine whether the foam backing, necessary for pre-deployed cell protection, should be left adhered to the substrate, reducing ϵ_{eff}, or retracted after panel deployment to allow for a higher ϵ_{eff}. The necessary thermal studies to be performed are outlined in the accompanying flow chart. (Ref: Figure 2.5.1)

Mention is made in the chart of a possible difference in ϵ_{eff} between white and black coatings on the substrate. (Note that, for example, bare Kapton emittance of approximately 75% leaves some room for improvement.) It is to be expected that a black ϵ_{eff} may be some 5% higher than the white. Other things being equal, this would mean, for no albedo input to the rear face, a difference of approximately $4^{\circ}F$ in cell temperatures, or on the order of a 1% higher power output from the "black" array. With albedo input to the rear array surfaces in near Earth orbits, power generation may be higher for the "white" even though both "black" and "white" power

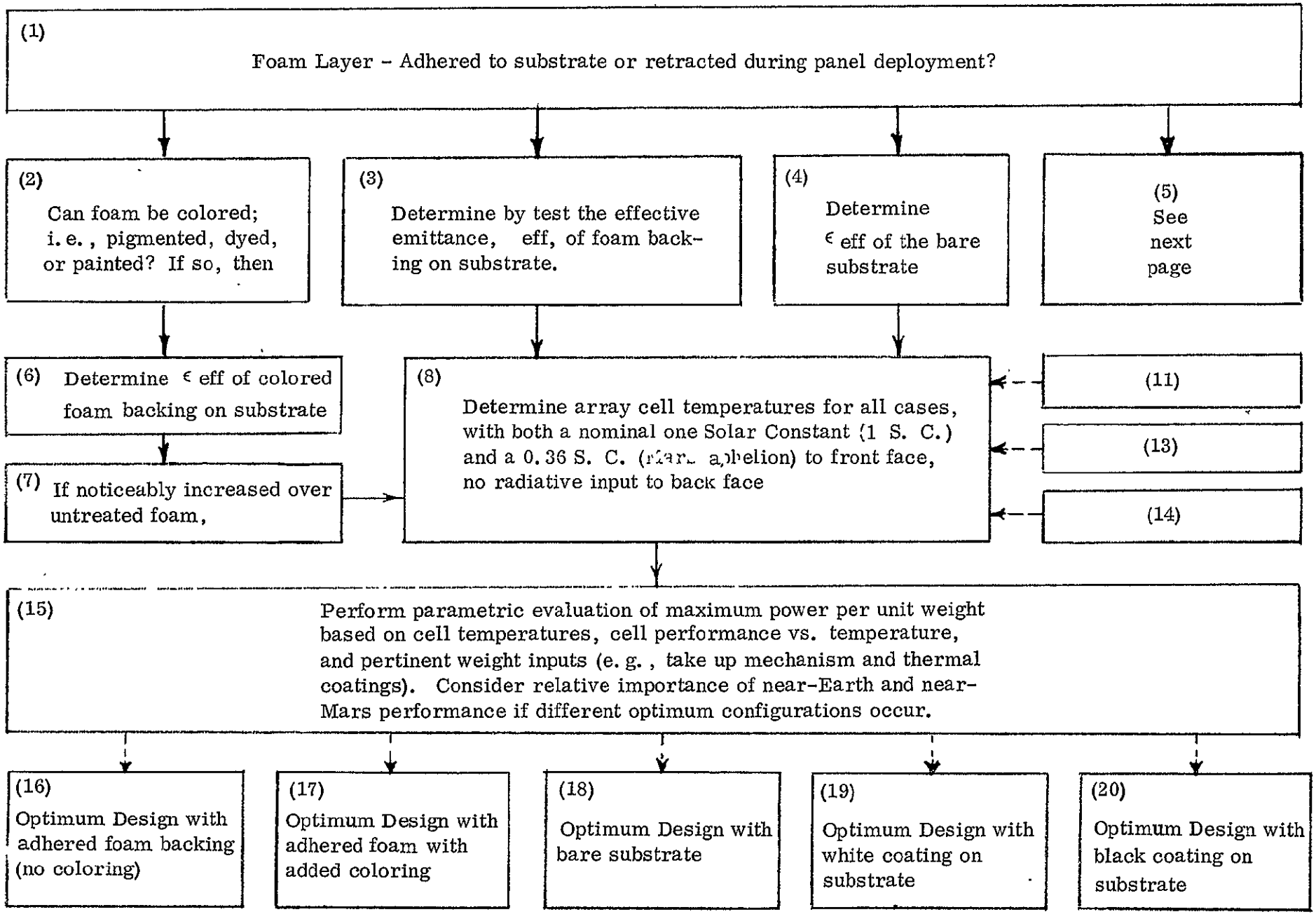

Flow Chart of Proposed Thermal Studies to Determine Optimum Configuration of Anti-Sun Substrate Surface

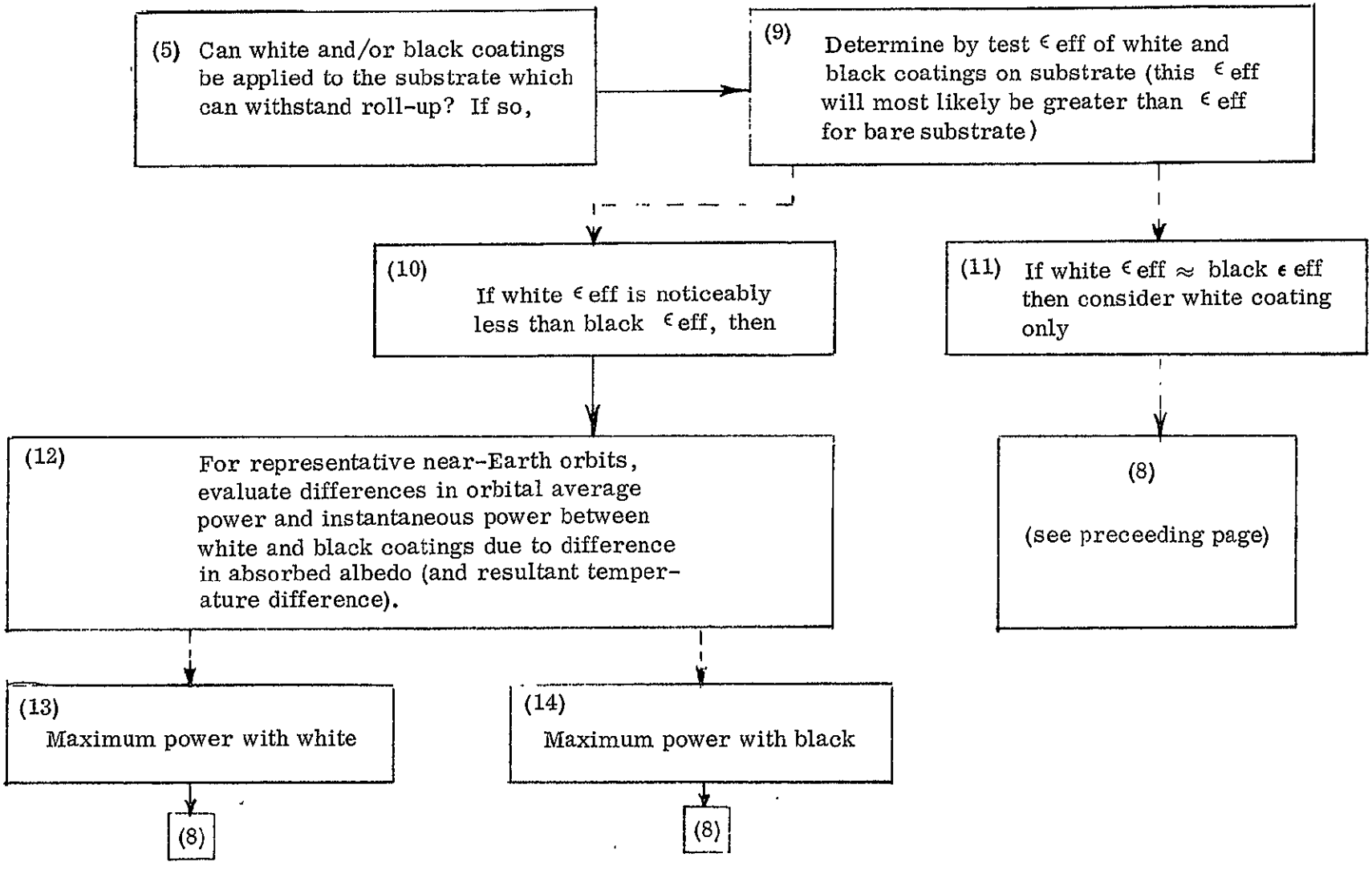

Note: Final conclusion is either (16), (17), (18), (19), or (20)

A dashed path represents one of a number of possible choices

Flow Chart of Proposed Thermal Studies to Determine Optimum Configuration of Anti-Sun Substrate Surface

outputs would most likely increase due to the albedo input to the front cell surface also. It is expected that the more critical power condition of far-from-Earth operation would mean that any advantage the white may have over the black close to Earth due to its lower absorptance would be negated if it suffers from a lower-than-black emittance. This white vs black is not thought to be applicable to the case of the foam backed substrate, since the rough texture of the foam surface implies essentially the same effective emittance for both white and black. Also, the solar absorptance of such a rough surface would not be so color dependent as, while being significantly greater than, a smooth surface of the same material. This same rough texture allows the possibility of the ϵ_{eff} of the uncolored foam being essentially equal to that of any colored foam.

2.5.3 Near-Mars Temperature Problems

So far, a majority of the thermal discussion has centered on the means of reducing cell temperature for maximum power-to-weight performance. However, as the spacecraft approaches 1.67 A.U. (Mars aphelion), low array temperatures, while still being welcomed with respect to power output, may present a materials problem when panel retraction is considered. For example, with average cell temperature at a hypothetical 110°F in the vicinity of the Earth (with no rear surface radiative input) a reduction of solar intensity to $\frac{1}{(1.67)^2}$, or 0.36 Solar Constants means a cell temperature drop to -19°F. This apparently not too severe temperature should cause no hesitiation in attempts at cell temperature reduction under near-Earth operation, since say an extra 10°F or 20°F reduction would still be most appreciated from a power viewpoint but cause little additional concern for materials failure.

It should be noted that attempts at panel retraction while the spacecraft is in the shadow of Mars should definitely be approached with caution, since the high area-emittance-product per unit-of-thermal-mass means extremely fast cool-downs in the absence of any appreciable radiative input. For example, an array initially at -19°F will drop to (approximately) -43°F one minute after going from full sun input to no-sun input, and to -145°F after 9 more minutes, and to -194°F after another 10 minutes. The rate of temperature decay will not be this severe in actuality, since the sun-no sun demarcation is softened due to the Mars penumbra.

However, it is obvious that extremely low temperatures can not be avoided in this instance of shadowing. While in Mars shadow, the only radiative inputs to the array are from Mars and spacecraft emitted I.R. energy. These inputs could be quite low, especially for a spacecraft position far from Mars (apogee in shadow) and low temperature and/or low emittance external spacecraft surfaces. Even in the case of Earth shadowing, low temperatures will also be of concern, although for near-Earth orbits, Earth I.R. emission will prevent array temperatures from falling below those experienced in Mars shadow. A typical lower limit for Earth orbits below 30,000 km might be on the order of $-180^{\circ}F$, while temperatures in Mars shadow may be in the vicinity of $-300^{\circ}F$.

2.5.4 Transient Temperature Behavior

As seen from the preceeding discussion, low shadowed-array temperatures are reached after rather sharp temperature decays: for the Mars shadow, on the order of $25^{\circ}F$/minute. For a sudden earth shadow (ignoring penumbra effects) starting with a $120^{\circ}F$ array, the rate of temperature drop is much more severe, at approximately $60^{\circ}F$/minute.

As the cold, dark array comes into the sun again, even higher rates of temperature change will occur. For example, an array at $-180^{\circ}F$ being suddenly illuminated with one Solar Constant will experience an initial rise of approximately $90^{\circ}F$/minute.

The aforementioned temperature transients will, if the array thermal mass estimate of .075 BTU/$^{\circ}F\ ft^2$ is correct, be extreme numbers since, for the purpose of a simple and conservative analysis, a sudden discontinuous step-change in solar energy was assumed. Actually, there will be a smooth, continuous transition from sun to dark, and vice versa, as the spacecraft passes through the planet's penumbra. Should the conservatively high estimates of temperature transients based on ignoring this penumbra effect cause any concern in the area of thermal shock, then a re-evaluation will be in order Using the array analytical thermal model and solar input vs. time based on a penumbra analysis, transient temperature histories will be recomputed. These temperature profiles will be continued throughout a maximum duration shadow trajectory (with thermal inputs from planet and spacecraft) to

determine minimum array temperatures.

2.5.5 Experimental Studies

In order to correctly evaluate the candidate external surfaces for the substrate, accurate estimates of effective thermal emittance are needed. This "effective" emittance will, when referenced to the cell temperature, include the effects of conductance through all material intermediate between cell and rear external surface. The most accurate and reliable means of obtaining such thermal emittance data is direct experimental measurement upon a thermal model which simulates as closely as possible the flight configuration. It is anticipated that the test program, to begin soon, will employ a set-up as sketched in cross section.

A large surface-to-edge area sample will minimize edge effects and will closely approach the desired one-dimensional model. Symmetry will insure that virtually all heat generated by the enclosed heater (uniformly distributed) will pass through the materials to be measured. The aluminum plates in this model simulate the solar cells; all other materials and adhesives will be as in flight.

Several thermal equilibrium conditions will be obtained through heater adjustment so that plate (i.e., cell) temperatures will cover the full expected cell temperature range. Average plate temperature and electrical power dissipation can then be measured and used to calculate an effective emittance for each temperature level for each of the candidate surfaces:

$$\epsilon_{eff} = \left(P_{dissip}\right) \div \left(A_{tot\ surface}\,\sigma\right) \left(T_{plate}\right)^4 .$$

No attempt will be made to measure surface or other interface temperatures due to the extreme difficulty in obtaining accurate temperature data on such low conductivity materials.

It would be extremely desirable to use aluminum plates and heater wire which duplicate the thermal mass of the actual cell assembly. Thus, turning off power after a steady state condition is reached (or reducing it in stages to simulate penumbra input) and then recording the temperature history will directly reveal the transient characteristics of the array. Likewise, transient heat up can be simulated,

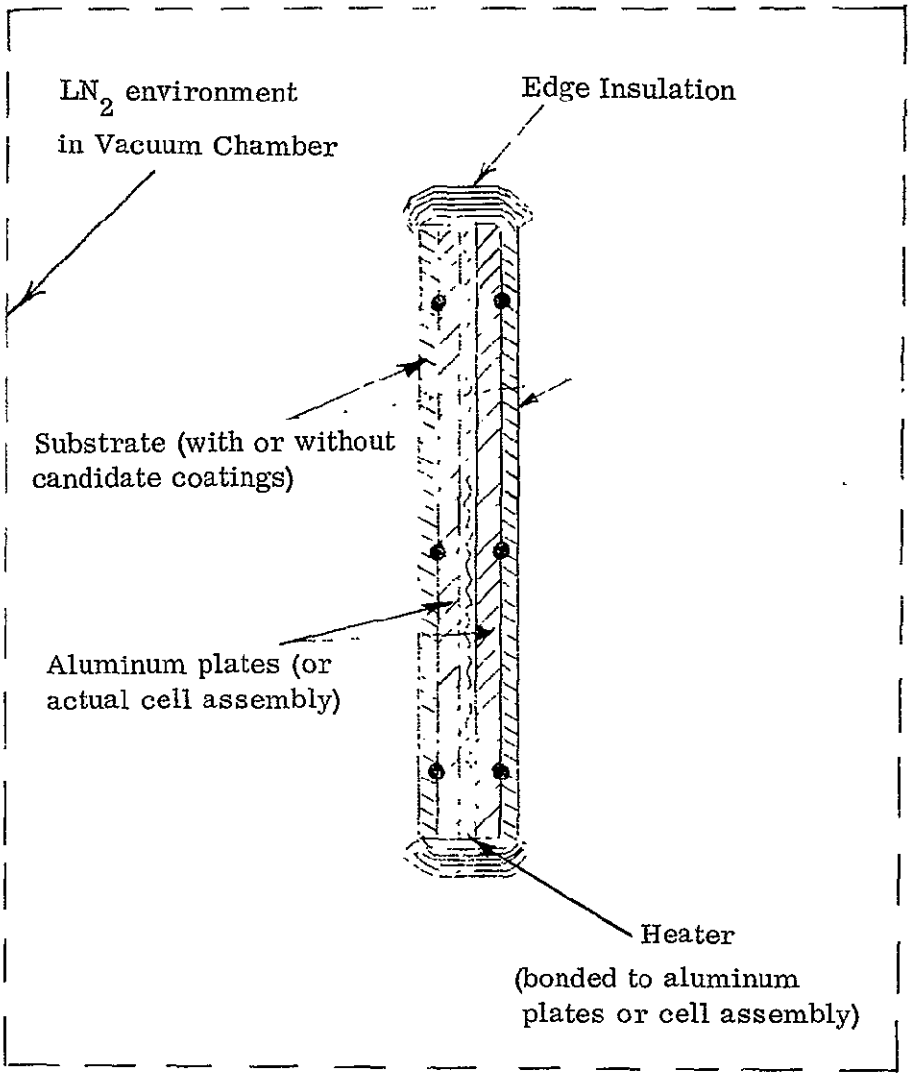

- Thermocouple Locations (attached to plates or cell assembly)

Cross-Section of Proposed Set-up for ϵ eff Test

beginning at a low temperature, by introducing heater power equivalent to the absorbed solar flux, based on a known value of solar absorbtance under cell electrical load.

If a realistic grouping of wired cells can be obtained in time for this test program, then it will be substituted for the aluminum plates in an effort to obtain more realistic transient data. Having this cell group and using the same general test set-up, the ϵ_{eff} of the array front surface should also be measured later in this program as a valuable check against assumed data.

2.5.6 Thermal Gradient Considerations

Under equilibrium solar illumination conditions, the array extension and support arms will be subjected to a thermal environment of infra-red radiation from the rear surface of the array substrate and "visible" spacecraft surfaces, and also conduction at the attachment ends. To minimize both the arm's absorbed energy from the array and its emitted thermal radiation, its external surfaces will be of minimum emittance. A polished metal surface or evaporatively deposited metal can yield an emittance on the order of 3%. Such a low value will mean that for a metal arm, conduction through the arm will be the predominant path for a relatively small quantity of heat flux, and temperature gradients, both circumferentically and longitudinally, will be greatly discouraged. Interior arm surfaces, ideally, should be optically black.

In near-Earth flight, there will at times be direct albedo input to the arms, with a resultant aggravation of thermal gradients since the absorptance of the metallic exterior arm surface may not be low enough to dismiss absorbed energy. It is believed that thermal distortions caused by any such resultant gradients are not so critical in the spacecraft's near-Earth trajectory (where power output is not so critical) and therefore need not be so closely predicted. Should a systems viewpoint deem this a possible problem area, however, this thermal condition can be readily analyzed.

At present, no temperature gradient problem in the support arms is anticipated, and such schemes as perforated arm material or super-insulation of arm surfaces would not be required.

If only thermal radiant energy from Sun and planet is considered, there will always be a uniformly distributed thermal flux on all surfaces of the (fully deployed)array. As such, thermal gradients laterally through the array will be negligible. However, when the possibility of additional radiant input from the spacecraft is considered, array surfaces may be receiving non-uniform fluxes. For example, external spacecraft surfaces which the array front surfaces view could, if their solar reflectance is finite, allow reflected solar energy (and to a smaller extent, albedo and earth emission) to strike only certain portions of the array. While this of course would be most welcome with respect to solar cell power output if the illumination pattern so allows, it would result in lateral temperature gradients, essentially localized at the boundaries of the various incident flux fields. If the nature of the array assembly and substrate material properties allows no thermal strain to develop, as appears likely, then this would be of minor concern.

However, candidate array configurations will be examined under the worst possible non-uniform flux condition, which, in the absence of exact spacecraft external surface shape and properties, is taken to be an area of variable, indeterminant size but with distinct line boundaries, superimposed on the array in a variable location, receiving an additional 100% of the normal incident solar flux.

3.0 CONCLUSIONS

The work accomplished during the reporting period has been concentrated in independent discipline investigations which are incomplete. Therefore, no conclusions as to the prime goal of the study, i.e., the feasibility of fabricating a 30 watt/pound roll-up solar array, can be drawn at this time.

4.0 RECOMMENDATIONS

Not Applicable.

5.0 NEW TECHNOLOGY

No reportable items.

6.0 REFERENCES

(1) Gunn, Langley, and Link (Texaco Experiment Inc., Richmond, Va.) Boron Filaments and Composites, Air Force - ASTM Symposium on "Standards for Filament Reinforced Plastic", Dayton, Ohio, 28pp., September 1966.

(2) Fiberglass Yarns, Owens-Corning, Toledo, Ohio, 33 pp. March 1955.

(3) Properties of Selected Commercial Glasses, Corning Glass Works, Corning, New York, 16 pp. January 1965.

(4) Borofil Adds Stiffness to Glass Fiber Plastics, TEIM-1025-1, Texaco Experiment Incorporated, Richmond, Va., 1 p., August 1967.

(5) Fiberglass Reinforced Plastics, Owens Corning, Toledo, Ohio, 33 pp. October 1961.

(6) Metallic Materials and Elements for Aerospace Vehicle Structures, MIL-HDBK-5A, DOD, Washington, D.C., 815 pp. February 1966.

(7) Aerospace Structural Metals Handbook Vol. 1, Air Force ASD-TDR-63-741 Wright-Patterson AFB, Ohio, March 1963.

(8) Unpublished data, Fairchild Hiller Corp., SESD.

(9) 18% Nickel Maraging Steels, International Nickel Co., New York, N.Y. 8 pp., March 1965.

(10) Kapton Polyimide Film, DuPont Bulletin H-2, Wilmington, Del., 8 pp.

(11) Metals Handbook, American Society for Metals, Metals Park, Novelty, Ohio, 1300 pp. 1961.

(12) Armco 17-7 PH, Armco Steel Corp., Middletown, Ohio, 10 pp.

(13) Faupel, Engineering Design, John Wiley and Sans, Inc., New York, 980 pp., 1964.

(14) Tsai and Azzi, Strength of Laminated Composite Materials, AIAA Journal Vol. 4 (2), February 1966.

(15) Schuerch, Prediction of Compressive Strength in Uniaxial Boron Fiber Metal Composite Materials, AIAA Journal Vol. 4 (1), January 1966

(16) Schwartz and Schwartz, Characteristics of Boron Fiber Reinforced Plastic Composites, AIAA Journal Vol. 5 (2), February 1967.

(17) Martin and Moore, R. and D. of Nondestructive Testing Technique for Composites, AFML-TR-66-270, Air Force Materials Lab. Feb. 1967